

# **PWM CURRENT CONTROLLED PERMANENT MAGNET BRUSHLESS DC MOTOR DRIVE FOR ELECTRIC VEHICLE APPLICATION**

**Major Project Report**

*Submitted in Partial Fulfillment of the Requirements for the degree of*

**MASTER OF TECHNOLOGY  
IN**

**ELECTRICAL ENGINEERING  
(Power Apparatus & Systems)**

By

**VIBHA SHARMA  
(05MEE017)**



**Department of Electrical Engineering  
INSTITUTE OF TECHNOLOGY  
NIRMA UNIVERSITY OF SCIENCE AND TECHNOLOGY  
AHMEDABAD 382 481**

MAY 2007

## **CERTIFICATE**

This is to certify that the Major Project Report entitled “PWM CURRENT CONTROLLED PERMANENT MAGNET BRUSHLESS DC MOTOR DRIVE FOR ELECTRIC VEHICLE APPLICATION” submitted by Ms. VIBHA SHARMA (05MEE017) towards the partial fulfillment of the requirements for the award of degree in Master of Technology (Electrical Engineering) in the field of Power Apparatus & Systems of Nirma University of Science and Technology is the record of work carried out by her under our supervision and guidance. The work submitted has in our opinion reached a level required for being accepted for examination. The results embodied in this major project work to the best of our knowledge have not been submitted to any other University or Institution for award of any degree or diploma.

**Date:**

### **Industry - Guide**

**Mr.Himanshu Swami**  
Assistant. Manager  
HEV Division  
Electrotherm India Ltd.  
Ahmedabad.

### **Institute - Guide**

**Dr. P.R.Upadhyay**  
Professor (E.E)  
Department of Electrical Engg  
Institute of Technology, Nirma University  
Ahmedabad.

**Head of Department**  
Department of Electrical Engineering  
Institute of Technology  
Nirma University  
Ahmedabad

**Director**  
Institute of Technology  
Nirma University  
Ahmedabad

*DEDICATED TO MY SON*  
*ANIRUDH*

## ACKNOWLEDGEMENT

Science always progresses from existing hypothesis and nothing originates from vacuum. Therefore, every work is always an effort of a group of individuals. The same is true for the present work also and it gives me an immense pleasure in acknowledging those who provided me guidance and help.

I feel indebted to **Dr. P. R. Upadhyay**, Professor, Department of Electrical Engg. Institute of Technology, Nirma University, Ahmedabad for his valuable suggestions and guidance throughout the thesis work. His critical insight and ingenious approach were vital to the progress of the project. I wish to express with felicity my gratitude to **Mr. Himanshu Swami**, Astt. Manager, R&D, HEV Department, Electrotherm India Ltd., for providing both practical and intellectual resources for the project.

With a sense of respect I express my solemn gratitude towards **Prof. B.B.Kadam**, Department of Electrical Engg. Institute of Technology, Nirma University, Ahmedabad who has been a constant source of encouragement.

I am thankful to **Mr.Priang Doshi** for suggesting a topic of contemporary interest. I gratefully acknowledge the cordial assistance provided by **Priyank, Pardeep** and **Nandish Bhai** from Furnance division, Electrotherm. **Mr. Atul Gupta, Mr.Kartik** and **Ms. Monali** from HEV department always offered practical solutions to my problems. I thank all my friends and colleagues who have been a source of strength.

Lastly, I extend my heartiest thanks to my family members for their moral support and encouragement without which the project would not have taken its present shape.

**Vibha Sharma**

## ABSTRACT

Electric Propulsion drives are gaining popularity as a technology for battery operated vehicles. This technology has the inherent advantage of energy conservation and being environmental friendly.

The objective of the present work is to design and develop a controller for Permanent Magnet Brushless DC (PMBLDC) Motor to be used in electric vehicle.

Based on the literature survey on the existing converter topologies and the control algorithm, VSI based PWM controlled PMBLDC Motor is proposed for the present study, the control algorithm has been implemented using hard switching. Since this algorithm can be effectively used in battery-operated drive and also provides the advantage of compactness.

PMBLDC Motor having a trapezoidal back *e.m.f* requires rectangular stator currents to produce constant torque. Because of non-sinusoidal variation of the mutual inductances between the stator and the rotor in PMBLDC motor, *abc* phase variable model is used for the modeling.

The control algorithm has been simulated and implemented. Implementation of the controller includes the design and fabrication of three-phase MOSFET based battery operated voltage source inverter and the control algorithm.

The control circuit has been fabricated using operational amplifier and logic gates. The control algorithm has been first verified for a 10  $\Omega$ , 500 W, star connected three-phase resistive load. Then after the control logic has been verified with PMBLDC motor. The phase displacement of the Hall position sensors has been determined. The accelerator output has been used to generate a PWM signal (1 kHz). The rotor position feedback and the PWM signal have been used to derive the switching commands for the six-inverter switches. By changing the modulation index at a given switching frequency of 1 kHz, the speed of the motor can be varied.

The proposed control algorithm is implemented on the resistive load and then it is applied to the PMBLDC motor under study. However the control strategy used in this work, results in high acoustic noise in the motor operation and this issue can be considered as a scope of further work.

## LIST OF FIGURES

Figure		Page
Figure. 1.1	Parts of Electric Vehicle	3
Figure. 1.2	BLDC Motor Drive Schematic for EV application	6
Figure. 3.1	Voltage Source Inverter BLDC Motor drive	12
Figure. 3.2	Phase back <i>e.m.f.</i> and phase current for BLDC Motor	12
Figure. 3.3	Gate waveforms for PAM strategy	14
Figure. 3.4	Gate waveforms for 120° switching	15
Figure. 3.5	Gate waveforms for 60° switching	16
Figure. 3.6	Gate waveforms for hard switching	16
Figure. 3.7	Schematic of the proposed controller	17
Figure. 4.1	Mathematical Model of three phase Inverter	20
Figure. 4.2	Three phase voltages as derived from mathematical model	20
Figure. 4.3	Line voltages as derived from mathematical model	21
Figure. 4.4	Equivalent Circuit Model of PMBLDC Motor	22
Figure. 4.5	Open loop response of PMBLDC Motor	23
Figure. 4.6	Trapezoidal back e.m.f as derived from Fourier series	23
Figure. 4.7	Mathematical model of PMBLDC Motor	24
Figure. 4.8	Mathematical model of one phase of PMBLDC Motor	24
Figure. 4.9	Phase Currents for PMBLDC Motor, derived from the Mathematical model	25
Figure. 4.10	Back e.m.f. for PMBLDC Motor, derived from the Mathematical model	25

Figure. 4.11	PMBLDC Motor torque ,derived from the Mathematical Model	26
Figure. 4.12	PMBLDC Motor Drive for Electric Vehicle	27
Figure. 4.13	Hall sensor output of the PMBLDC Motor(simulation)	28
Figure. 4.14	PWM signal for PMBLDC Motor Drive(simulation)	28
Figure. 4.15	Deriving Gate pulses for switch 1	29
Figure. 4.16	Deriving Gate pulses for switch 4	29
Figure. 4.17	Gate pulses for the Inverter switches	29
Figure. 4.18	Phase currents for PWM controlled PMBLDC Motor	30
Figure. 4.19	Phase voltages for PWM controlled PMBLDC Motor	30
Figure. 4.20	Speed, phase current and torque for PWM controlled PM BLDC Motor, ( $V_{\text{accel}} = 4.8\text{V}$ )	31
Figure. 4.21	Speed, phase current and torque for PWM controlled PM BLDC Motor ,( $V_{\text{accel}} = 4\text{V}$ )	32
Figure. 5.1	Schematic of the control circuit	34
Figure. 5.2	Deriving the PWM signal-implementation	35
Figure. 5.3	Pin Diagram of IR 2110	37
Figure. 5.4	Schematic of the Dead time logic	39
Figure. 5.5	Dead Time between the complimentary switches-implementation	40
Figure. 5.6	Hall position sensor output of the PMBLDC Motor	40
Figure. 6.1	The developed control circuit for PWM controlled PMBLDC Motor	42
Figure. 6.2	Hall sensor output and the inverted signal for PMBLDC Motor	43
Figure. 6.3	Logic for generating dead time between the complimentary Switches	43

Figure. 6.4	Output of the dead time circuit	44
Figure. 6.5	Generating the gate pulse for the Inverter switches	44
Figure. 6.6	Gate pulses for complimentary switches, at the Input of the MOSFET gate driver	45
Figure. 6.7	Gate pulses for high side switches, at the Output of the MOSFET gate driver	45
Figure. 6.8	Control circuit and the power module for PWM controlled PMBLDC Motor	46
Figure. 6.9	Line voltage for resistive load ,at battery voltage of 36V	47
Figure.6.10	Phase voltage for resistive load, at battery voltage of 36V	47
Figure. 6.11	Phase voltage for resistive load, at 36V,modulation index=1	48
Figure.6.12	Complete experimental set-up of PWM controlled PMBLDC Motor Drive for Electric Vehicle	49



## LIST OF TABLES

<b>Table</b>		<b>Page</b>
Table: 1	Characteristic of BEV, HEV, and FCEV	2
Table: 2	Evaluation of EV motors	5
Table: 3	Application of EV motors	6
Table: 4	Characteristics of Sinusoidal Brushless Motor and Trapezoidal Brushless Motor	11
Table: 5	Comparison between MOSFET and IGBT	36
Table: 6	Comparison between MOSFET drivers	37
Table: 7	Observed Inverter output at different battery voltages	48
Table: 8	Observed rotor speed for different stator voltages	49

## NOMENCLATURE

<b>Symbol</b>	<b>Definition</b>	<b>Units</b>
$\omega_r$	rotational speed of motor	<i>r.p.s.</i>
$L_a$	armature inductance per phase	Henry
$R_a$	armature resistance per phase	$\Omega$
$I_a$	armature current	Ampere
$E_a$	back <i>e.m.f.</i>	Volts
$V_a$	Terminal voltage	Volts
$T_e$	motor torque	N-m
$J$	moment of inertia	$\text{kg-m}^2$
$V_{DSS}$	Maximum drain to source voltage	Volts
$I_D$	Drain current	Ampere

## CONTENTS

<b>Acknowledgement</b>	<b>i</b>
<b>Abstract</b>	<b>ii</b>
<b>List of Figures</b>	<b>iii</b>
<b>List of Tables</b>	<b>vi</b>
<b>Nomenclature</b>	<b>vii</b>
<b>Chapter 1: INTRODUCTION</b>	<b>1-6</b>
1.1 General	1
1.2 Development of Electric Vehicles	1
1.3 Electric Vehicle Configurations	1
1.4 Battery Electric Vehicle	3
1.4.1 Energy source for Battery Electric Vehicles	3
1.4.2 Power Converter for Battery Electric Vehicles	4
1.4.3 Electric Motor for Battery Electric Vehicles	4
<b>Chapter 2: LITERATURE SUTVEY</b>	<b>7-9</b>
2.1 General	7
2.2 Motor Drive for Electric Vehicles	7
2.3 Control Algorithm for PMBLDC Motor Drive	7
2.4 Switching Strategies for PMBLDC Motor Drive	8
2.5 Modeling and Simulation of PMBLDC Motor Drive	8
2.6 Conclusions	9

<b>Chapter 3: PERMANENT MAGNET BRUSHLESS DC</b>	
<b>MOTOR DRIVE SYSTEM</b>	<b>10-18</b>
3.1 General	10
3.2 Permanent Magnet Brushless DC Motor	10
3.3 Operating Principle of a PMBLDC Motor Drive System	11
3.4 Brushless DC Motor Drive Strategies	13
3.5 Conclusions	18
<b>Chapter 4: MATHEMATICAL MODELING AND</b>	
<b>SIMULATION OF PWM CONTROLLED</b>	
<b>PMBLDC MOTOR DRIVE</b>	<b>19-33</b>
4.1 General	19
4.2 Mathematical Model of Three Phase Inverter	19
4.3 Mathematical Model of PMBLDC Motor	21
4.4 PMBLDC Motor Drive for Electric Vehicle	26
4.4 Simulation Results	28
4.5 Conclusions	33
<b>Chapter 5: HARDWARE DEVELOPMENT OF PWM</b>	<b>34-41</b>
<b>CONTROLLED PMBLDC MOTOR DRIVE</b>	
5.1 General	34
5.2 Development of Triangular Wave Generator	35
5.3 Selection of Switching Device	35
5.4 Development of Gate Driver for MOSFET	36
5.5 Operation of Bootstrap Circuit	38

5.6 Selection of Bootstrap Components	38
5.7 Dead Time Logic	39
5.8 Determination of the Hall Sensor's Displacement	40
5.9 Conclusions	41
<b>Chapter 6: PERFORMANCE OF PWM CONTROLLED PMBLDC MOTOR DRIVE</b>	<b>42-50</b>
6.1 General	42
6.2 Execution and Development of the Control Circuit	42
6.3 Performance of the Inverter with Resistive Load	45
6.4 Performance of the Inverter with the PMBLDC Motor used for Electric Vehicle	48
6.5 Conclusions	50
<b>Chapter 7: MAJOR CONCLUSIONS AND SCOPE FOR FURTHER WORK</b>	<b>51-52</b>
7.1 General	51
7.2 Major Conclusions	51
7.3 Scope for Further Work	52
<b>References</b>	<b>53-55</b>
<b>Appendix</b>	<b>56</b>
I. Specifications of the Motor under study	
II. Fourier Series Representation of trapezoidal back <i>e.m.f.</i>	

# CHAPTER 1

---

## INTRODUCTION

### 1.1 General

In the present world where energy conservation and environment protection are growing concerns the development of electric vehicle technology has taken on an accelerated pace. Electric Vehicle (EV) is a road vehicle that involves with electric propulsion. Electric propulsion is to interface electric supply with vehicle wheels transferring energy with high efficiency under the control of the driver during the ride. The Electric Vehicle configurations and the general considerations regarding the components of EV are discussed.

### 1.2 Development of Electric Vehicles

Electric Vehicle was invented in 1834. A number of companies in U.S.A., U.K. and France produced EVs during the last decade of the 19<sup>th</sup> century. However, due to the limitations associated with the batteries and with the advancement of internal combustion engine vehicles, EVs almost vanished since 1930.

In the early 1970s, energy resources crisis and environmental concerns compelled rekindling of interests in EVs. Although EVs did well in the late 1990s, they are still in the research and development stage. Many advanced technologies are being employed to extend the speed range and reduce the cost of the vehicle. The development of electric propulsion systems has been based on the growth of various technologies; mainly in the field of electric motors, power electronics, and microelectronics and control strategies. In the next few decades, it is anticipated that EVs will be commercialized and they will have their market share.

### 1.3 Electric Vehicle Configurations

The main components of the electric vehicle are electric motor, controller, power converter and a source of power. The general considerations regarding each of the components are discussed in the following section.

Depending on the source of power used Electric Vehicles are categorized as Battery Electric Vehicles (BEVs), Hybrid Electric Vehicles (HEVs), and Fuel Electric Vehicles (FEVs).

*Battery Electric Vehicles:* are energized by an on board battery.

*Hybrid Electric Vehicles:* are energized by more than one source of power one of which is essentially an electric source.

*Fuel Cell Electric Vehicles:* utilizes fuel cells as the source of power. Fuel cell is an electrochemical device that converts the free- energy of an electrochemical reaction into electric energy. In contrast to a battery, the fuel cell generates energy rather than storing it, and continues to do so as long as the fuel supply is maintained.

The source of power in case of BEVs is the on board battery, therefore they are mainly suitable for short-range, low-speed vehicles; which require a smaller battery size. HEVs can provide higher speeds but they have a higher cost as compared to BEVs. FCEVs have a long-term potential but cost and refueling systems are the major concerns.

The major characteristics of these three types of vehicles are given in table 1.

*Table- 1 Characteristics of BEV, HEV and FCEV*

<i>Types of EVs</i>	<i>Battery EVs</i>	<i>Hybrid EVs</i>	<i>Fuel Cell EVs</i>
<i>Propulsion</i>	Electric motor drives	Electric motor drive Internal combustion engines	Electric motor drives
<i>Energy system</i>	Battery Ultra capacitor	Battery Ultra capacitor ICE generating unit	Fuel cells
<i>Characteristics</i>	Zero emission Independence on crude oils Short range (100-200km) Commercially available	Very low emission Dependence on crude oils Long driving range Commercially available	Zero emission Independence on crude oils Satisfied driving range Under development
<i>Major issues</i>	Battery management Charging facilities	Managing multiple energy sources Battery sizing and management	Fuel cell cost Fuel processor Fueling system

The main focus for the present study has been on battery electric vehicles.

### 1.4 Battery Electric Vehicle

It has been indicated by the above discussion that Battery electric vehicles are successful for short speed-range and are becoming popular because of environmental and energy conservation concerns. The present work has been dedicated to the development of motor drive for battery electric vehicle. The major parts of a BEV are

1. Battery.
2. Power converter.
3. Electronic controller.
4. Electric motor.

Block diagram of the battery electric vehicle is as shown in Fig. 1.1

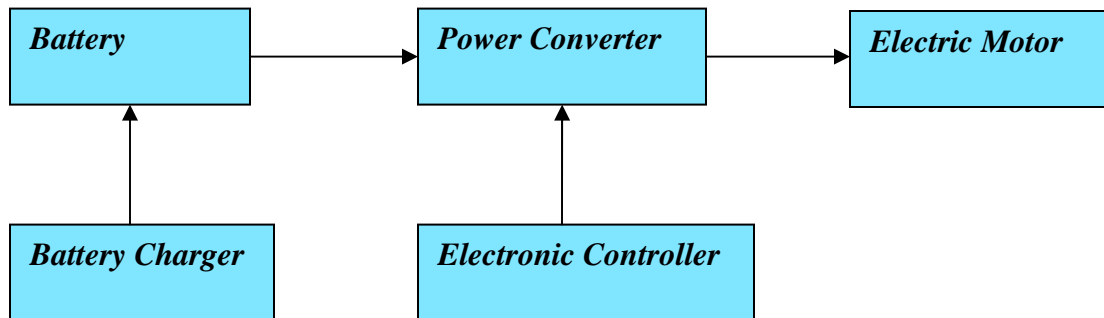


*Fig.1.1 Parts of Battery Electric Vehicle*

The general considerations regarding the components of BEV have been discussed in The following section:

#### 1.4.1 Energy Source for Battery Electric Vehicles

The source of power for battery electric vehicle is the on board battery. The general criteria for the development of the batteries for vehicle application are summarized as:

1. High specific energy and energy density.



2. Fast charging and deep discharging capabilities.
3. Long cycle and service lives.
4. Maintenance free.
5. Re-cycleable.

Based on the above consideration, the viable options for EV batteries are VRLA, Ni-Cd, Nickel-zinc, and sodium/sulphur.

#### **1.4.2 Power Converter for Battery Electric Vehicles**

The power converter employed for BEV has to be compact and is also required to deliver high power density and high efficiency. DC-DC converters and DC-AC converters are employed for DC and AC motors respectively. In addition to the conventional pulse width modulated (PWM) inverters, resonant dc-link inverters are also gaining popularity as one of the latest inverter topologies for battery –fed applications. The direction of rotation, speed and torque delivered by the motor is controlled by switching sequence of the power devices.

#### **1.4.3 Electric Motor for Battery Electric Vehicles**

The electric propulsion system is the heart of EV; it consists of the motor drive, transmission device and wheels. The electric motor to be used in an electric vehicle should be small in size and should have a high efficiency. Due to space constraints, the motor must have a short axial length. Major requirements of EV motor drive are summarized as follows

1. High power density.
2. High torque at low speeds for starting and climbing.
3. Very wide speed range including constant torque and power regions.
4. High efficiency over wide speed and torque ranges.
5. Fast torque response.
6. High reliability and robustness for various vehicle-operating conditions.
7. Reasonable cost.

Traditional dc commutator motors (dc motors) have been prominent in EV propulsion, because their torque –speed characteristics suit traction requirement well and their speed controls are simple. However, the dc motor has a commutator, hence it requires

regular maintenance. As high reliability and maintenance –free operation is prime considerations for electric propulsion in EVs, commutatorless motors are becoming attractive. Induction Motors (IM) is widely accepted commutatorless motors for EV, as they are highly reliable and free from maintenance. Alternatively PM Brushless motors are also promising because they use permanent magnets to produce the magnetic field. . Hence higher efficiency and high power density can be achieved.

The evaluation of motors for electric vehicle is shown in table 2 in which a point grading system is adopted where five points are referred as the best measure. [1-3]

*Table- 2 Evaluations of EV Motors*

	<i>DC motor</i>	<i>Induction motor</i>	<i>PM Brushless motor</i>
<i>Power density</i>	2.5	3.5	5
<i>Efficiency</i>	2.5	3.5	5
<i>Controllability</i>	5	4	4
<i>Reliability</i>	3	5	4
<i>Cost</i>	4	5	3
<i>Total</i>	17	21	20

Because of highest efficiency and higher controllability PM Brushless motor have been successfully applied to electric vehicles. The advantages of PM Brushless motor are summarized as follows.

1. Since the magnetic field is excited by high energy permanent magnets, the overall weight and volume can be significantly reduced for a given output power, leading to higher power density.
2. Because of the absence of rotor copper losses, their efficiency is inherently higher than that of IMs.
3. Since the heat mainly arises in the stator, it can be more easily dissipated to surroundings.
4. PM excitation inherently offers higher reliability.
5. Because of lower electromechanical time constant of the rotor, acceleration at a given input power can be increased.

The market trends in electric propulsion technology also indicate that PMBLDC Motor is a promising candidate for Electric Vehicles. The type of motor drives used in some popular EV models [1] has been listed in Table-3.

*Table- 3 Applications of EV Motors*

<i>Sr.NO</i>	<i>EV models</i>	<i>EV motors</i>
1	Honda EVPlus	PM Brushless motor
2	Nissan Altera	PM Brushless motor
3	Toyota RAV4	PM Brushless motor
4	YO Smart	PM Brushless motor
5	Ford Think City	Induction motor
6	GM EVI	Induction Motor

The above discussion strongly supports the application of PMBLDC motor for electric vehicles. The schematic for BLDC motor drive developed for the present study is as shown in Fig.1.2

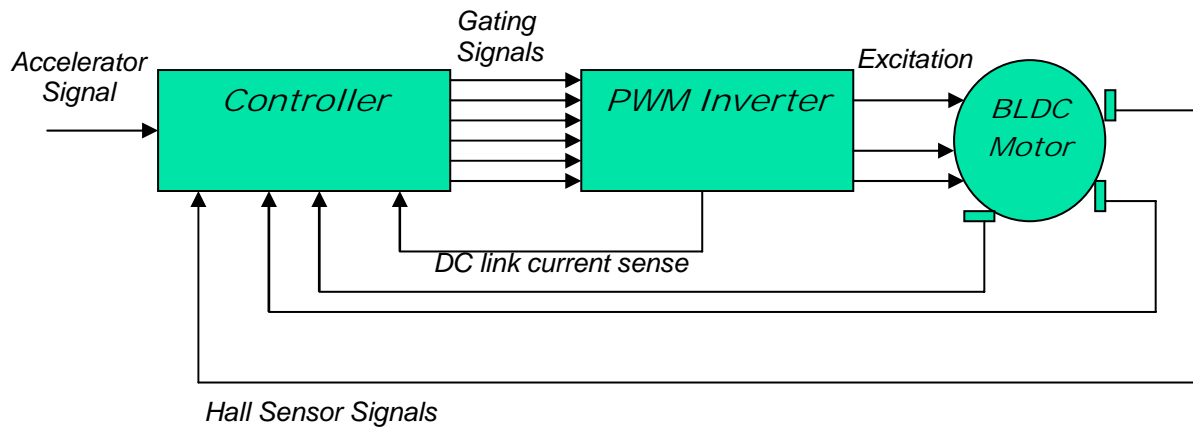


*Fig. 1.2 BLDC motor drive schematic for EV application*

The torque command is derived from the accelerator. The accelerator signal and the rotor position feedback are used by the controller to derive the gating signals for the inverter switches. The inverter output provides the required excitation to the stator of BLDC motor.

## CHAPTER 2

---

### LITERATURE SURVEY

#### 2.1 General

The main source of reference for the present study has been the IEEE transactions on Industry Application, Industrial Electronics, Power Electronics and the Proceedings of the IEEE. Literature survey has been carried out about the motor drive for the Electric Vehicle, Control Algorithm for PMBLDC motor and the power converter topology. For the implementation part Application Notes from International Rectifiers have also been referred. A few references are being discussed while a detailed list of all the references has been given at the end of the thesis.

#### 2.2 Motor Drive for Electric Vehicle

[1] C.C.Chan

**“The State or the Art of Electric and Hybrid Vehicles”**. It has been concluded that Permanent Brushless DC (PMBLDC) motors has been prominent in electric propulsion because their torque-speed characteristics suit traction requirement well and their speed controls are simple.

[2] C.C.Chan, K.T. Chau

**“An Overview of Power Electronics in Electric Vehicles”**. It has been concluded that the PWM inverters, resonant dc-link inverters and dc-dc converters (choppers) are the commonly used power converter topologies.

#### 2.3 Control Algorithm for PMBLDC Motor Drive

[3] Z.Q.Zhu, Y.Liu, D. Howe

**“Comparison of Performance of Brushless DC Drives under Direct Torque and PWM Current Control”**. The major inference drawn is that the low frequency torque ripple is less for Direct Torque Control technique.

[4] M.K. Jamil, N.A. Demerdash

**“Harmonics and Core Losses of Permanent Magnet DC Motors Controlled By Chopper Circuits”**. It has been concluded that for Chopper driven Permanent Magnet DC Motors the core losses increase significantly.

[5] Bhim Singh, B.P. Singh, K. Jain

**“Implementation of DSP Based Speed Controller for Permanent Magnet Brushless dc Motor”**. It has been concluded that fast and compact controller for PMBLDC Motor can be implemented by sensor less control employing DSP.

#### **2.4 Switching Strategies for PMBLDC Motor Drive**

[6] H. Tan, S.L. Ho

**“A Novel Single Current Sensor Technique Suitable for BLDCM Drives”**.

Two major conclusions drawn are: In a BLDC Motor Drive system the inverter works in the 120° conduction mode and the PWM strategies generally used are double-sided PWM, single-sided PWM or double-sided complimentary PWM.

#### **2.5 Modeling and Simulation of PMBLDC Motor Drive**

[7] P. Pillay, R. Krishnan

**“Modeling of Permanent Magnet Motor Drives”**. It has been concluded that because of trapezoidal back *e.m.f.* and the non-sinusoidal variation of the motor inductances, phase variable approach is used for modeling of PMBLDC Motor.

[8] P. Pillay, R. Krishnan

**“Modeling, Simulation, and Analysis of Permanent –Magnet Motor Drives, Part-II: The Brushless DC Motor Drive”**. The trapezoidal back *e.m.f.* can be either generated using the piece-wise linear approach or represented by Fourier series.

## 2.5 Conclusions

The important conclusions drawn from the literature survey have been summarized as:

1. PM Brushless Motors have been successfully applied to Electric Vehicles.
2. PM Brushless Motor provides a good pick-up to the Electric Vehicle, but limits the speed range of the vehicle
3. Because of the interaction between trapezoidal back *e.m.f.* and the rectangular phase currents the torque produced by PM BLDC Motor is higher than its AC counterpart.
4. Inverter for BLDC Motor operates in 120° conduction mode.
5. Current Source Inverter used as a power converter provides inherent regenerating capability, but the overall system becomes bulky. Therefore Voltage Source Inverter employed in vehicle applications.
6. The number of switches per phase can be reduced to reduce the overall size and cost of the system; this however makes the control strategy complex.
7. For Chopper driven PM Brushless Motor Drives the core losses are significantly high.
8. PWM and Direct Torque Control are the commonly used algorithms for PM Brushless Drives.
9. More precise and fast control can be implemented by eliminating the position sensors and detecting the zero crossing of the back *e.m.f.* However a high-speed processor is inevitable in this case.
10. Since the rotor inductances are non-sinusoidal, phase variable approach is used for modeling of PM Brushless DC Motor.

## CHAPTER 3

---

# PERMANENT MAGNET BRUSLESS DC MOTOR DRIVE SYSTEM

### 3.1 General

Permanent Magnet Brushless DC (PMBLDC) motors are the direct current motors with permanent magnets on the rotor and armature windings on the stator. These motors have better efficiency, better power factor and a greater output power, because the field excitation is contributed by the permanent magnets. The principle of operation, power converter topology and the control strategies for PMBLDC motor drives has been discussed.

### 3.2 Permanent Magnet Brushless DC (PMBLDC) Motor

A brushless dc motor is a dc motor turned inside out, i.e. the field is on the rotor and the armature is on the stator. The torque-current characteristics of a brushless dc motor mimic that of the dc motor. Instead of commutating the armature current using brushes, electronic commutation is used. Having the armature on the stator makes it easy to conduct heat away from the windings. The most obvious advantage of these motors is the removal of brushes, leading to the elimination of many problems associated with brushes. Another advantage is the ability to produce a larger torque at the same peak current and voltage, because of interaction between rectangular current and rectangular magnetic field. Moreover the brushless configuration allows more cross-sectional area for the armature windings thereby facilitating the conduction of heat from the frame and hence, increasing the electric loading and power density.

PMBLDC motor drives require variable-frequency, variable –amplitude excitation that is usually provided by a three-phase inverter. The inverter is responsible for both electronic commutation and current regulation, the position information obtained from the position sensors is used to open and close the six switches of the inverter.

Depending on the interconnections of the stator windings and hence the type of the back *e.m.f.*, two types of constructions are possible-trapezoidal and sinusoidal motors. [29]

Although their configurations are very similar, there is a distinct difference in that PM brushless dc (PMBLDC) motors are fed by rectangular ac wave, while PM synchronous (PMSM) motors are fed by sinusoidal or PWM ac wave. A comparison between the characteristics of PMBLDC motors and PMSM motors has been carried out in table-4.

*Table- 4 Characteristics of Sinusoidal Brushless Motor and Trapezoidal Brushless Motor*

<i>Characteristic</i>	<i>Sinusoidal Brushless Motor</i>	<i>Trapezoidal Brushless Motor</i>
<i>Air gap flux distribution</i>	Sinusoidal	Trapezoidal
<i>Back e.m.f.</i>	Sinusoidal	Trapezoidal
<i>Excitation Current</i>	Sinusoidal	Square wave or quasi-square-wave
<i>Position Sensor</i>	Uses Continuous rotor position feedback signals to control commutation.	Uses discrete rotor position feedback signals for commutation.
<i>Torque output</i>	Lower	Higher

### **3.3 Operating Principle of PMBLDC Motor Drive System**

A conventional PMBLDC drive is illustrated in Fig.3.1. It consists of a rectifier arrangement, a dc link capacitor for energy storage, a Voltage Source Inverter (VSI). The three-phase output of the inverter is supplied to the motor. Although not explicitly shown, for position sensing purposes, either a Hall position sensor or an optical shutter arrangement is used. In order to achieve a constant torque that is ideally free from ripple, the desired current is a rectangular ac wave, 120° broad. A profile for each phase of the motor with respect to the corresponding back-*e.m.f.s* as a function of the rotor position is shown in Fig.3.2, at each rotor position, a constant current multiplies the constant part of the back-*e.m.f.*; hence the sum of the products of a phase back-*e.m.f.* and the corresponding phase current is constant.



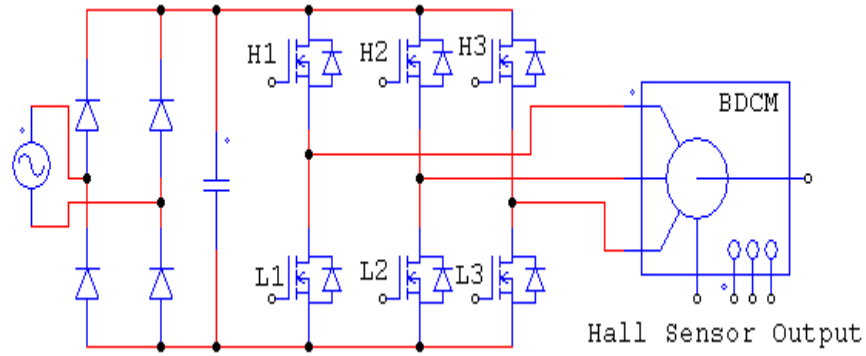


**Fig.3.1 Voltage source inverter BLDC Motor drive**

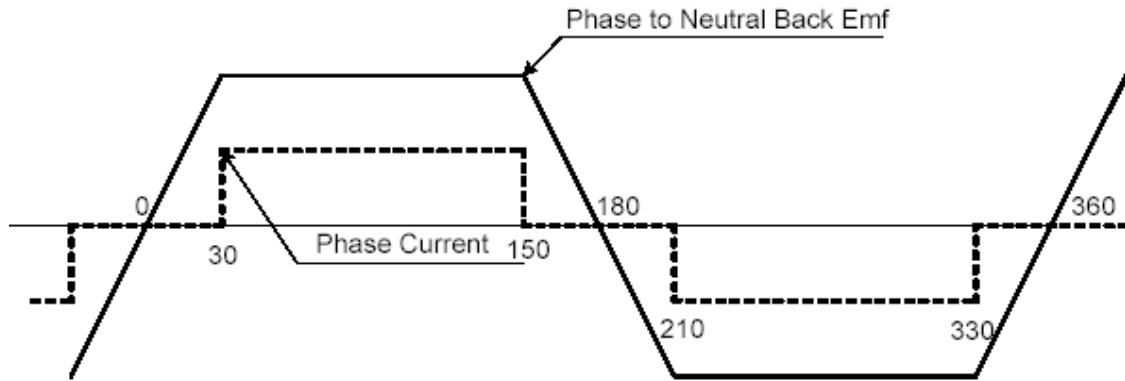


**Fig.3.2 Phase back e.m.f. and phase current of PMBLDC Motor**

The desired current profile is achieved by supplying the PMBLDC motor from either a VSI or a Current Source Inverter (CSI). When using a VSI, the desired current profile is achieved by controlling the switching of the transistors. The natural shape of the current supplied by a CSI conforms to the desired profile. At any given time, only two switches out of the six switches of an inverter are conducting. This means that only two phases are conducting at any instant, with current entering one of the phases and leaving through the other, as can be seen from Fig.3.2 there is a definite relation between the back-*e.m.f.s* and the current waveforms, as a function of the rotor position. Hence, in order to have proper operation of this motor, it is necessary to synchronize the phase currents with the phase back-*e.m.f.s*. This is achieved by the use of Hall position sensors, which detect the position of the

rotor field, and hence the position of the rotor shaft. [4] [5]. A motor with synchronized switching is able to produce a positive torque.

The phase currents and the back *e.m.f.* can be synchronized either by using a voltage source inverter (VSI) or a current source inverter (CSI) as the power converter [6- 7]. In case of voltage source inverter both bipolar switching based drives and unipolar switching based drives are commonly used [8-11]. In case of current source inverter, rectifier and current source inverter topology is employed.

Since the source of power in case of EV is the on board battery, VSI is the proposed topology for the power converter. The motor under study will be controlled in the constant torque region by using the PWM controlled stator currents and voltage source inverter.

### **3.4 PM Brushless DC Motor Drive Strategies**

Speed control can be implemented by varying the average voltage across the stator windings. This tends to change the value of the average stator current. However for a constant load torque, the stator current has to be maintained constant. Hence the back *e.m.f.* induced in the stator windings have to change such that the stator current remains constant. This accounts for change in speed (as the field is being supplied by permanent magnet), thus increasing the stator voltage increases the motor speed. Various techniques to vary the average stator voltage in case of Brushless DC Drive have been discussed [12] as follows:

#### **1. Pulse Amplitude Modulation**

In this strategy, varying the magnitude of the bus voltage changes the voltage across the motor windings. A boost converter is used with a diode rectifier. This strategy is quite efficient and simple. The waveforms for this strategy are shown in Fig.3.3

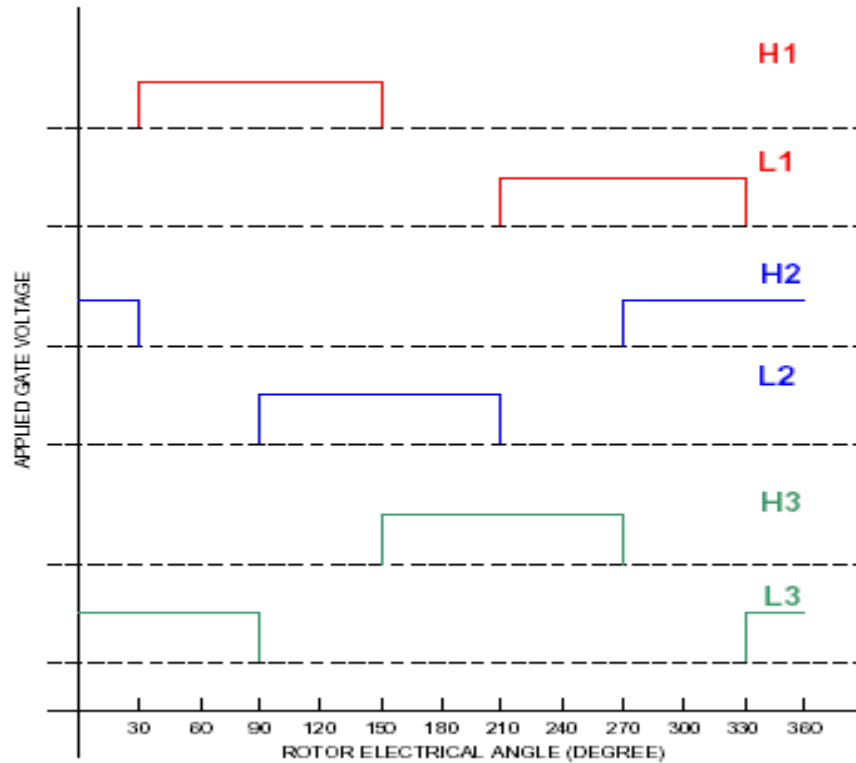


*Fig.3.3 Gate waveforms for PAM*

As is seen that each switch is ON continuously for an angular duration of  $120^\circ$ , in one complete electrical rotation. The ON times of the two switches in the same phase are displaced from each other by  $120^\circ$ . In this strategy the switch power loss is only due to conduction.

## 2. Pulse Width Modulation

The voltage applied across the motor windings can also be changed by modulating switch duty cycle within the conduction interval. In this case, the DC bus voltage is kept constant. Output voltage can be controlled either by switching one switch per leg or by switching both the switches, accordingly the following PWM strategies can be implemented:

### a. $120^\circ$ Switching

In this case only one-switch is modulated per leg while the other conducts. The high side switch modulates the duty cycle and the low side switch provides current for  $120^\circ$  duration as shown in Fig.3.4.

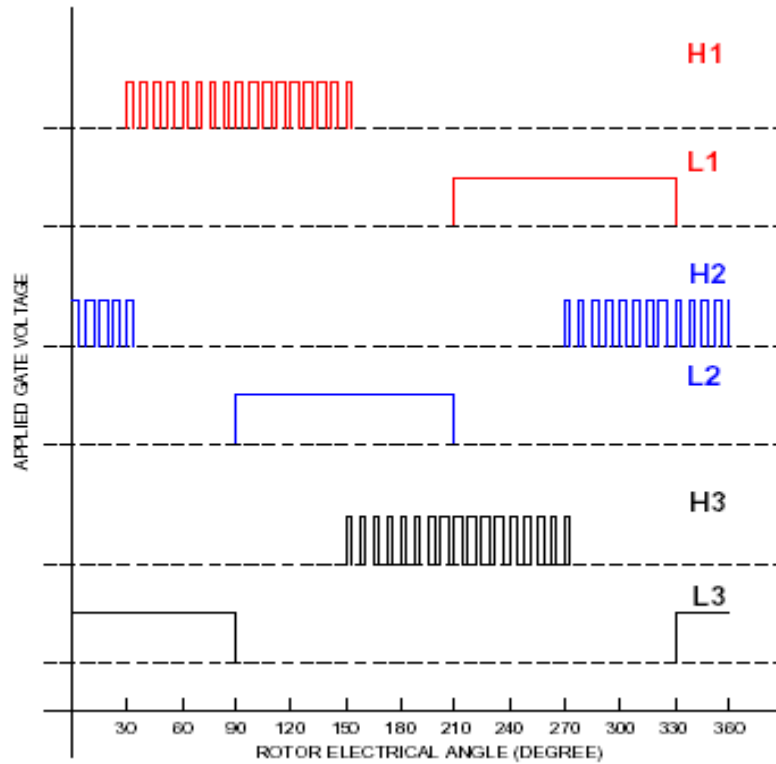


*Fig.3.4 Gate waveforms for 120° PWM switching*

In this strategy apart from the conduction losses, switching losses are also significant. Secondly, loss distribution between switches is not uniform. While the low side switches have only conduction losses, the high side switches have both switching and the conduction losses. Also, since the body diodes of the MOSFET conduct during off time of the high side switch, the diode conduction and reverse recovery losses are non-trivial.

b. 60° Switching

In this strategy both the high side and the low side switches are switched for 60° electrical as shown in Fig. 3.5. In this case power losses are distributed symmetrically, between the high and low side switches. Also as in 120° switching the high side and low side diodes have non-trivial power losses.

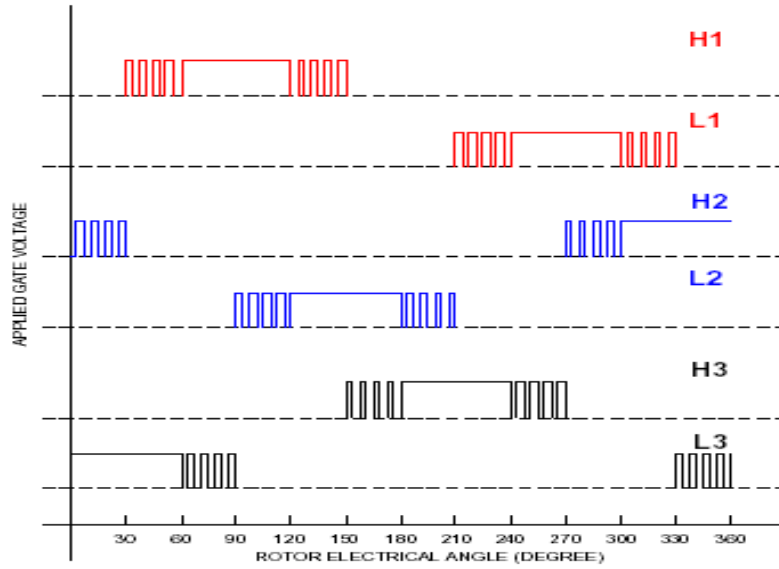


*Fig 3.5 Gate waveforms for 60° PWM switching*

c. Hard Switching

In this strategy, both the high side and the low side switches are modulated simultaneously, as shown in Fig.3.6.

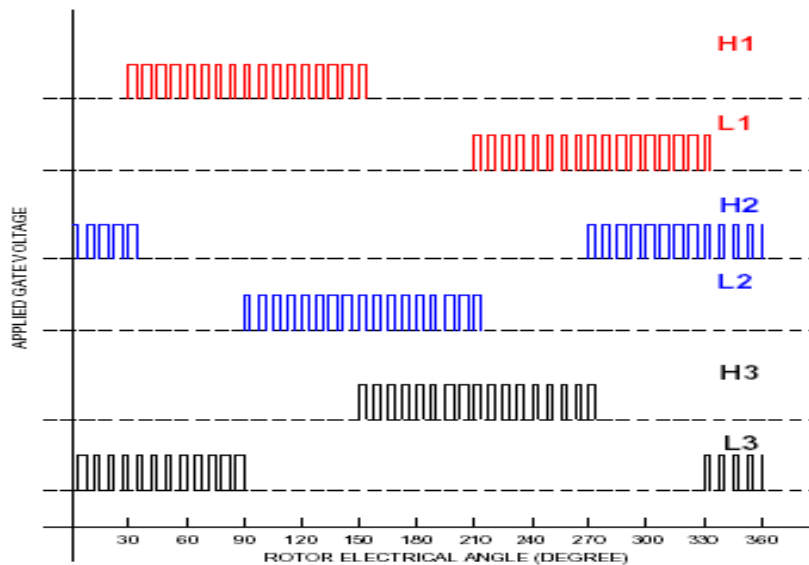


*Fig. 3.6 Gate waveforms for hard switching*

As indicated by the gate waveforms neither the high-side switch nor the low-side switch conducts continuously. The conduction losses are reduced as compared to  $120^\circ$  switching and  $60^\circ$  switching. Since the switching is symmetrical, power losses are equally distributed between the switches.

The motor under study has been controlled in the constant Torque region by using the PWM controlled stator currents and voltage source inverter. The present study employs hard switching for controlling the speed of the motor. The overall schematic for the proposed drive is as shown in Fig.3.8

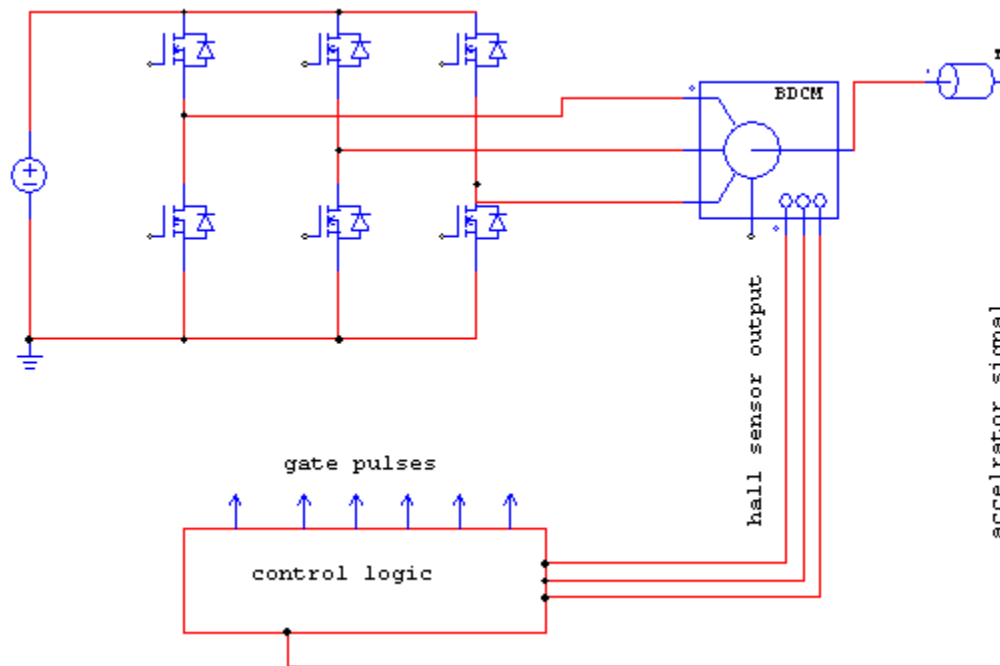


*Fig. 3.8 Schematic of the proposed controller*

### 3.5 Conclusions

It has been concluded from the above discussion that the PM Brushless DC Motor:

1. Produces larger torque because of the interaction between rectangular current and rectangular magnetic field.
2. Requires a variable frequency, variable amplitude excitation.
3. Electronic commutation and current regulation is carried out by the three-phase inverter.
4. Phase currents and back *e.m.f.* are synchronized by taking rotor position feedback from the Hall position sensors.
5. Phase currents and back *e.m.f.* are synchronized by taking rotor position feedback from the Hall position sensors.
6. Phase currents and back *e.m.f.* are synchronized by taking rotor position feedback from the Hall position sensors.
7. Speed control can be implemented by varying the average voltage across the stator windings.
8. The control strategies commonly employed are Pulse Amplitude Modulation and Pulse Width Modulation.
9. Pulse Width Modulation can be implemented either by 120° switching, 60° switching or by hard switching
10. Since the source of power in case of EV is the on board battery, VSI has been proposed as the power converter topology and hard switching has been employed as the switching technique.

## CHAPTER 4

---

# MATHEMATICAL MODELING AND SIMULATION OF PWM CONTROLLED PMBLDC MOTOR DRIVE

### 4.1 General

In this chapter the mathematical model of PMBLDC Motor and the circuit level simulation of the control algorithm is discussed. The rotor inductances in case of PMBLDC motor are non-sinusoidal; therefore *abc* phase variable approach has been used for the mathematical modeling. Mathematical modeling of the system has been carried out using Matlab Simulink software package [12]. The control algorithm has been simulated using circuit simulator PSIM.

### 4.2 Mathematical Model of the Three Phase Inverter:

The mathematical model of the inverter has been derived by using the PWM technique. The output of the inverter equals  $V_{dc}$  or  $-V_{dc}$ , according to the position of the switch of a particular phase. The line voltages have been calculated by using the following equations:

$$V_{ab} = (S_a - S_b)V_{dc};$$

$$V_{bc} = (S_b - S_c)V_{dc}$$

$$V_{ca} = (S_c - S_a)V_{dc};$$

where  $S_a, S_b, S_c$ , indicates the switch position.  $V_{ab}, V_{bc}, V_{ca}$  are the line voltages for the three phase inverter and  $V_{dc}$  is the dc link voltage.

From the above equations the phase voltages have been calculated as follows:

$$V_{an} = (V_{ab} - V_{ca})/3;$$

$$V_{bn} = (V_{bc} - V_{ab})/3;$$

$$V_{cn} = (V_{ca} - V_{bc})/3;$$

where  $V_{an}, V_{bn}, V_{cn}$  are the phase voltages



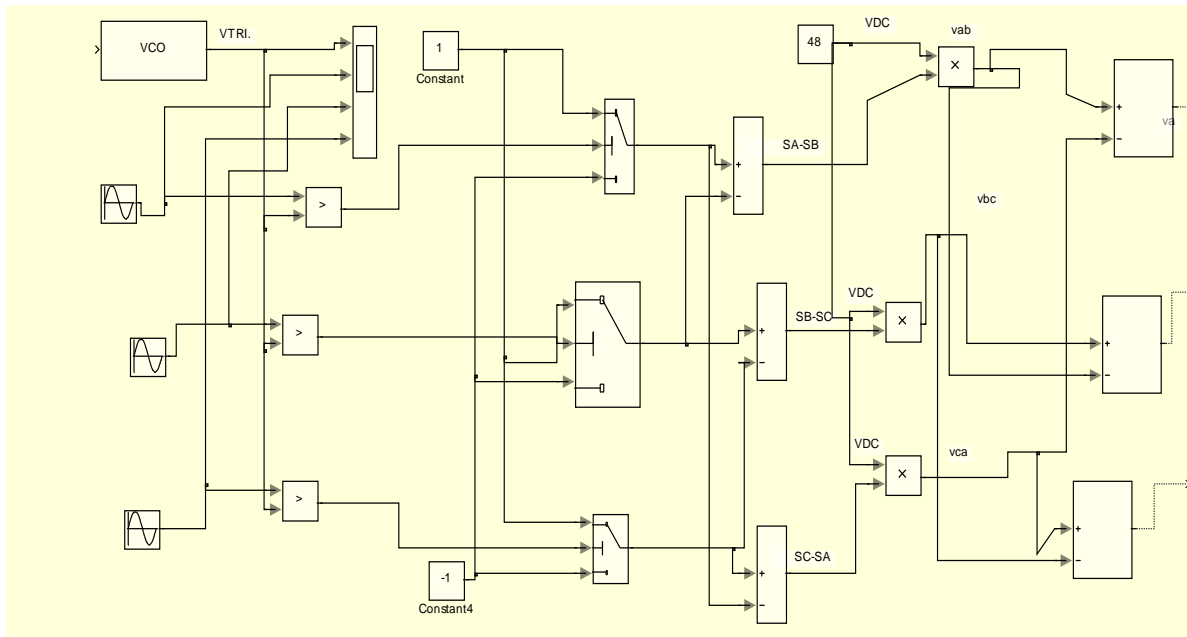


**Fig. 4.1 Mathematical Model of three Phase Inverter**

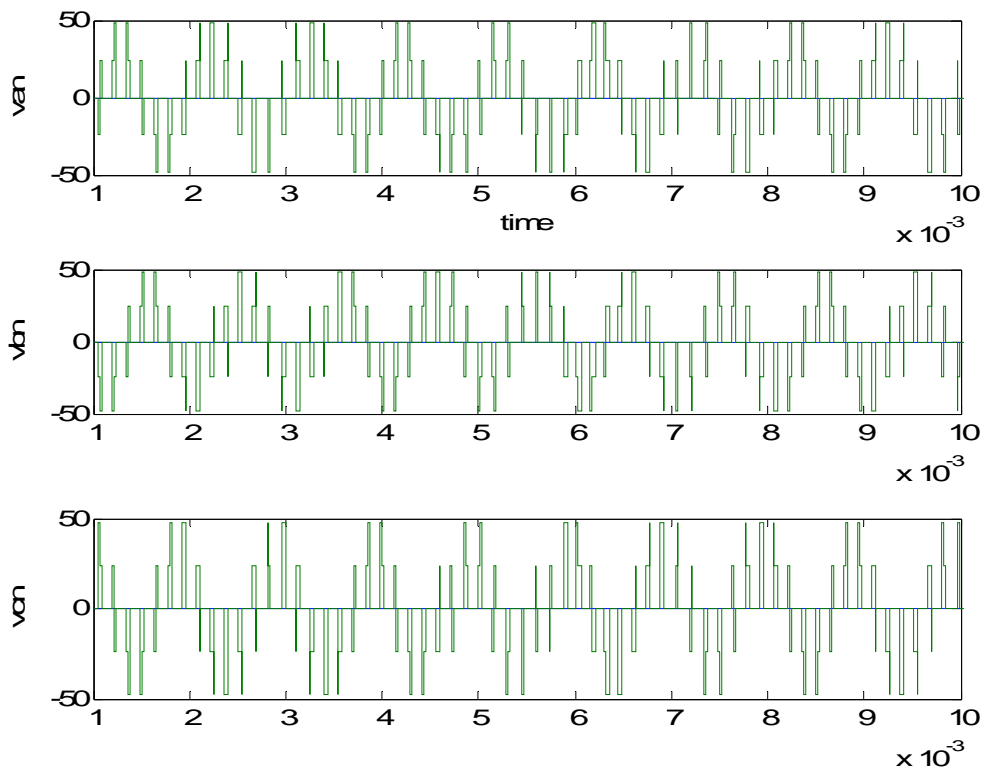


**Fig.4.2 Phase voltages of inverter as derived from mathematical model**

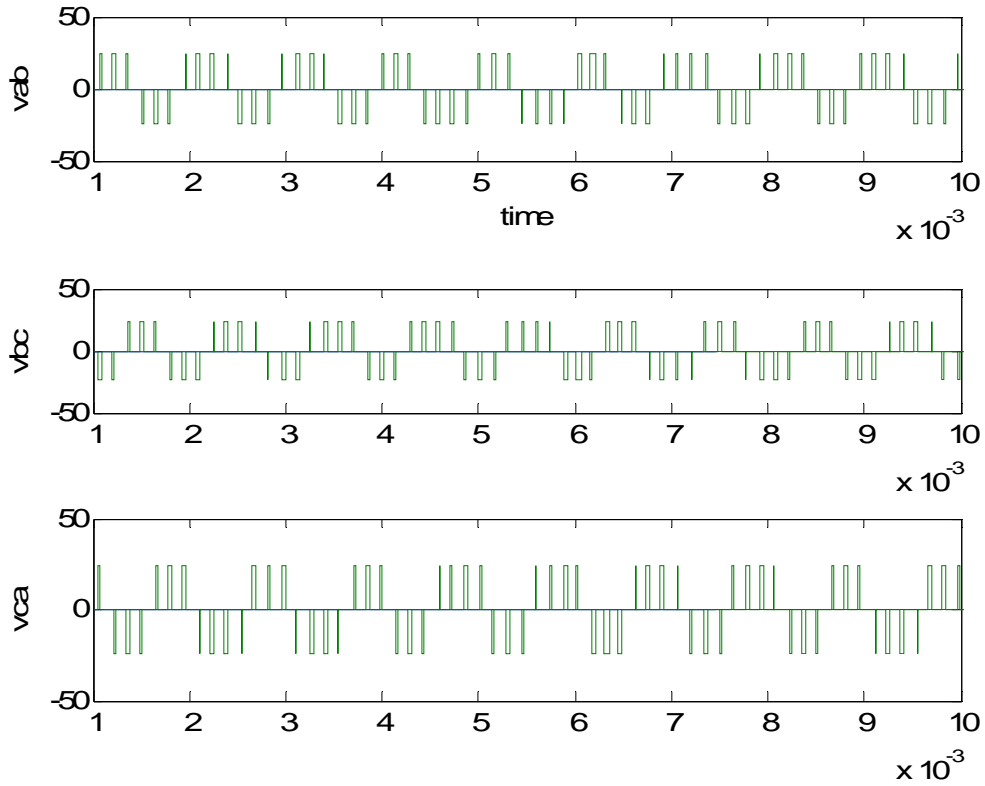


*Fig.4.3 Line voltages for the inverter as derived from mathematical model*

### 4.3 Mathematical Modeling of Permanent Magnet DC Motor.

In the Permanent Magnet Brushless DC (PMBLDC) Motor, since the back *e.m.f* is non sinusoidal, the inductances do not vary sinusoidally in the *abc* frame and it does not seem advantageous to transform the equations to the *d,q* frame since these inductances will not be constant after transformation .Hence *abc* phase variables model is used . [13-16].

Equations used for the modeling of PMBLDC motor are

$$V_a = Ri_a + L \frac{di_a}{dt} + E_a$$

$$V_b = R i_b + L \frac{di_b}{dt} + E_b$$

$$V_c = Ri_c + L \frac{di_c}{dt} + E_c$$

Where R=the per phase resistance;

L=the per phase inductance;

$E_a, E_b, E_c = a, b, c$  phase back *e.m.f.* ;

The electromagnetic torque is given by the equation;

$$T_e = (E_a i_a + E_b i_b + E_c i_c) / \omega_r$$

The equation of motion is as follows;

$$\partial \omega_r = (T_e - T_l - B \omega_r) / J$$

Parameters of the motor used for modeling, [4] are shown below;

$$R = 0.315 \text{ ohm}$$

$$L = 3.4 \text{ mH}$$

$$K_t = 2.3 \text{ kg}$$

$$K_e = 0.24 \text{ V/r.p.m.}$$

$$J = 0.0032 \text{ kg-m}^2$$

$$b = 0.0024 \text{ N/rad/s}$$

the open loop response of the motor has been observed. The model used to study the open loop response is as shown in Fig 4.4

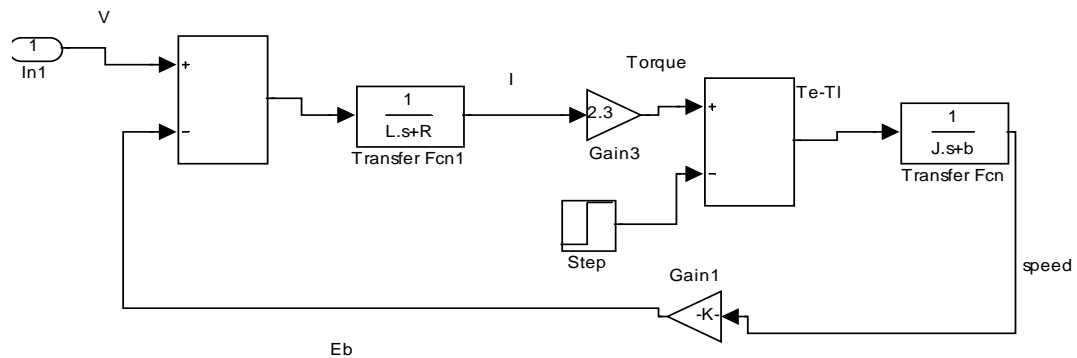


**Fig.4.4 Equivalent Circuit Model of PMBLDC Motor**

The open loop response for a step change in load, shown in Fig.4.5 indicates that BLDC is an inherently stable system.

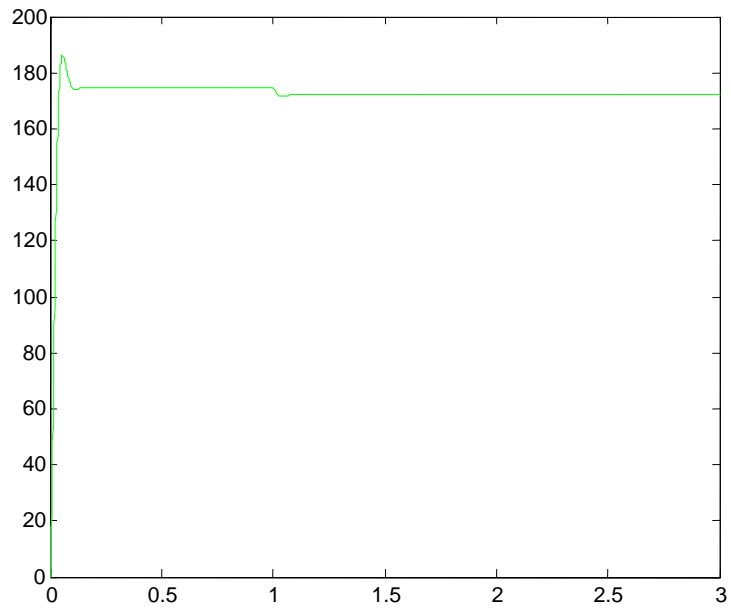


**Fig. 4.5 Open loop response of PMBLDC Motor**

The derivation of the mathematical model of PMBLDC motor requires the calculation of the back *e.m.f.*. The back *e.m.f.*'s for PMBLDC Motor is a function of rotor position and is trapezoidal in shape. By using Fourier series and assuming a unity magnitude of the *e.m.f.*, The variation of the back *e.m.f.* is found to be as shown in Fig.4.6

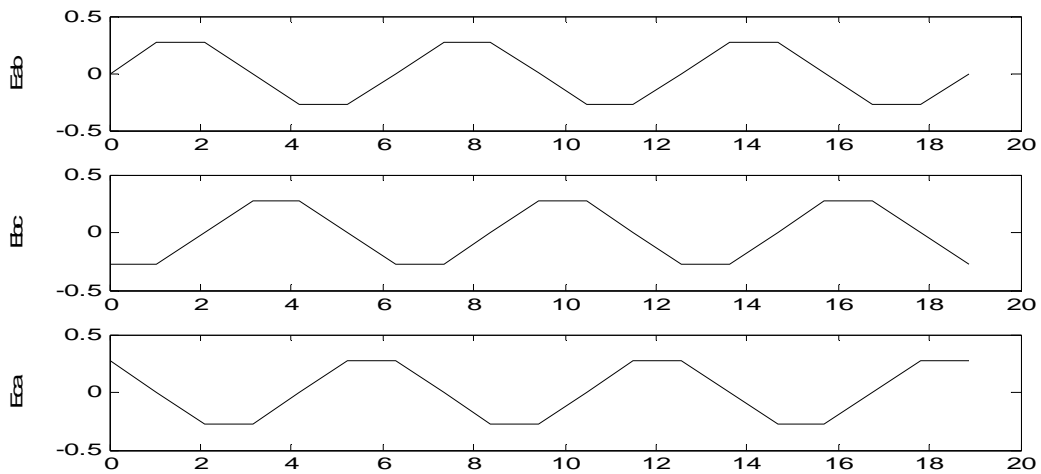


**Fig.4.6 Trapezoidal back e.m.f. as derived from Fourier series**

The mathematical model of PMBLDC Motor is derived by using the equations mentioned early in this section and is as shown in Fig. 4.7

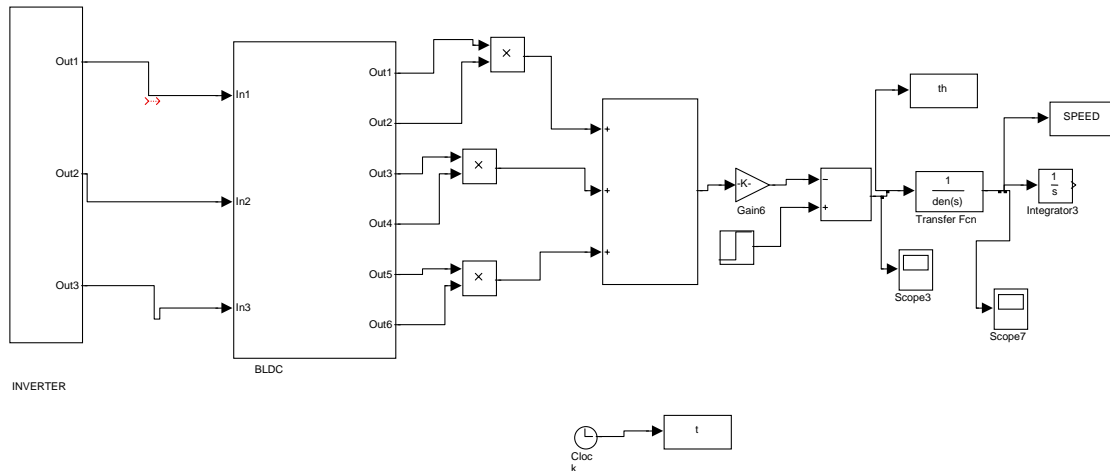


**Fig. 4.7 Mathematical model of PMBLDC Motor**

The block “BLDC” in the figure includes three individual single phase circuits representing each phase. The single phase diagram is as shown in Fig.4.8.

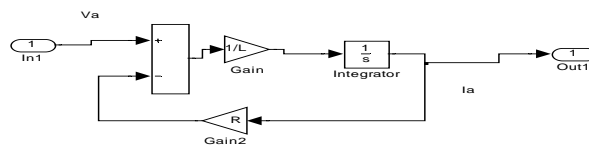


**Fig.4.8 Block diagram for one phase of BLDC Motor**

The signals Out1, Out3, Out5 indicate the phase current and the signals Out2, Out4, Out6 indicate the back e.m.f. of the three phases. The “INVERTER” block represents the three phase inverter

The Phase currents, back *e.m.f* and motor torque obtained from the mathematical model are shown in Fig.4.9, Fig.4.10 and Fig.4.11 respectively.

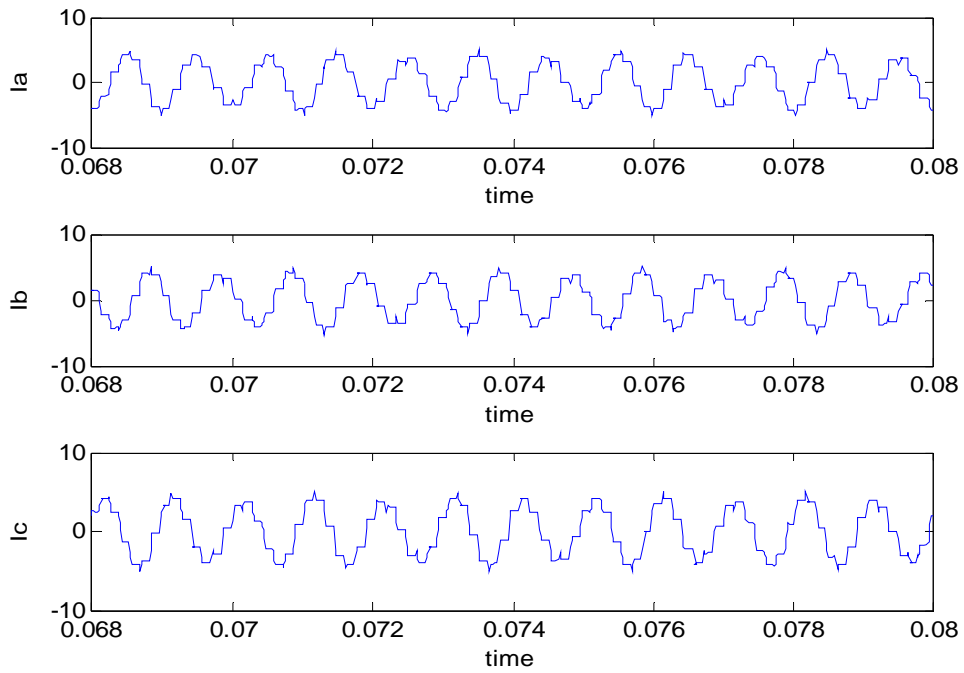


**Fig. 4.9 Phase Currents for PMBLDC Motor, derived from Mathematical Model**

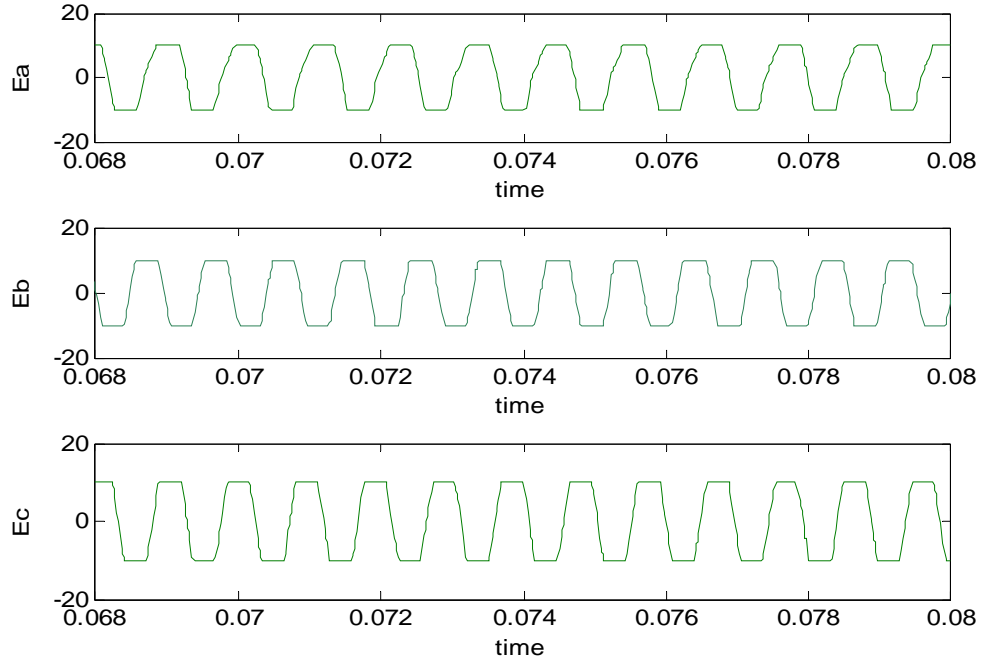


**Fig.4.10 Back e.m.f.s for PMBLDC Motor, derived from Mathematical Model**

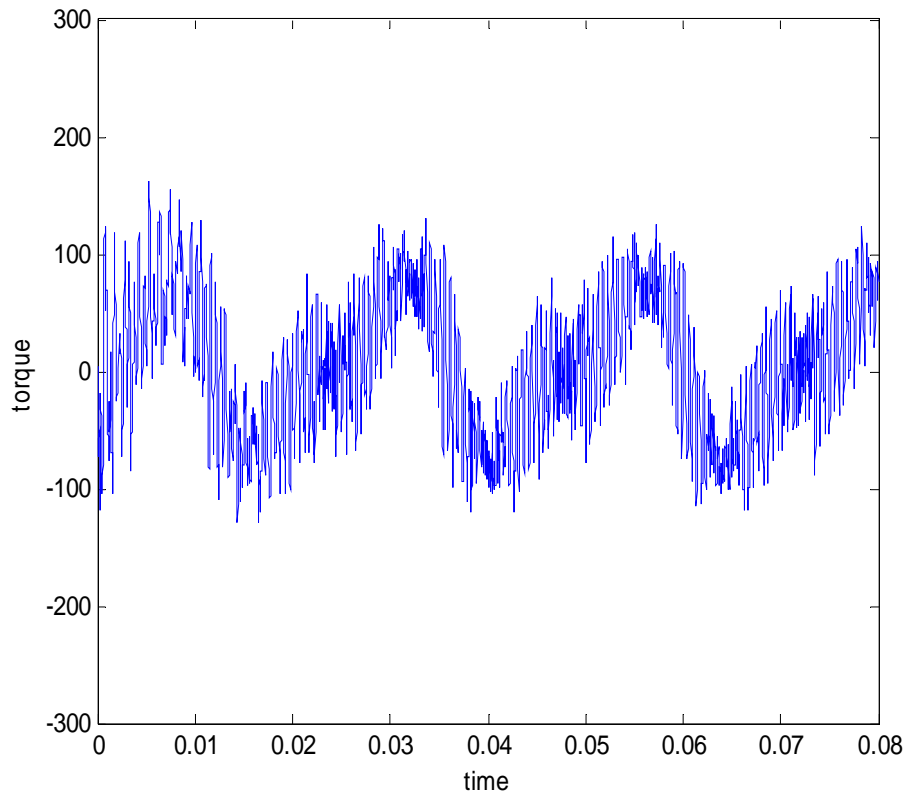


*Fig. 4.11 PMBLDC Motor torque as derived from mathematical model*

#### **4.4 PMBLDC drive for Electric Vehicle**

The three phase currents for PMBLDC are derived from square wave inverter. For vehicle applications the control signals are derived from the accelerator position and the Hall sensor output. The circuit diagram for implementing the proposed control algorithm and to carry out the simulation is as shown in Fig. 4.12

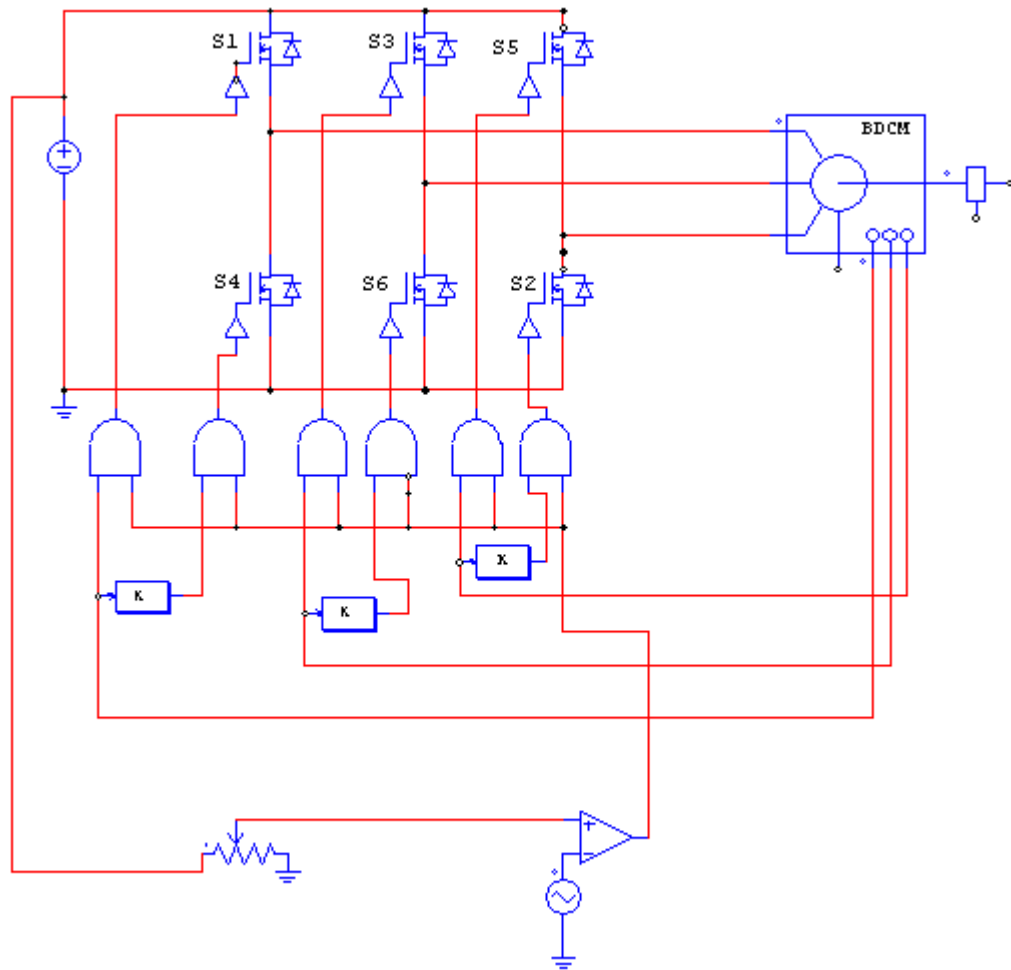


*Fig.4.12 PMBLDC Motor drive for Electric Vehicle*

The accelerator signal has been found to be a dc voltage of varying amplitude (4.3-0.8V). This signal is compared with a triangular wave of 1 kHz to generate PWM signal. The rotor position signals are combined with the PWM signal to generate the gate pulses for the six-inverter switches.



## 4.5 Simulation Results

The simulation of the control algorithm was performed using the circuit simulator PSIM. The simulation results are as follows, the speed, torque and the phase currents for two different positions of the accelerator are shown.

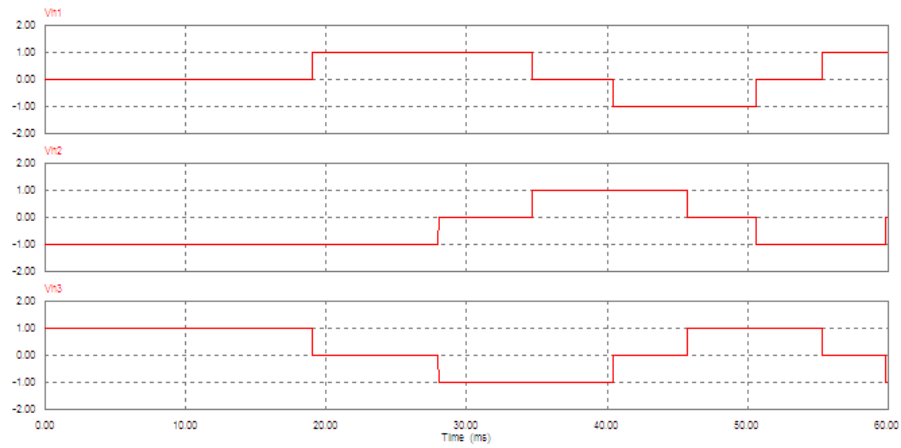


*Fig.4.13 Hall sensor output of the PMLDC Motor (simulation)*

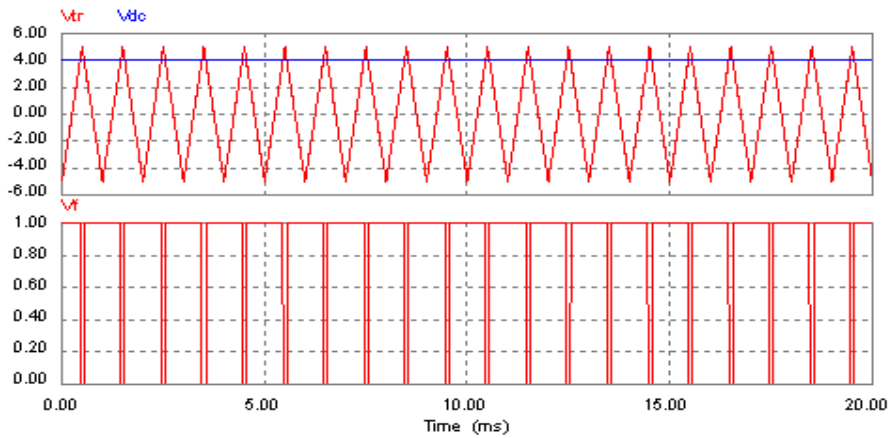


*Fig. 4.14 PWM signal for PMLDC Motor (simulation)*

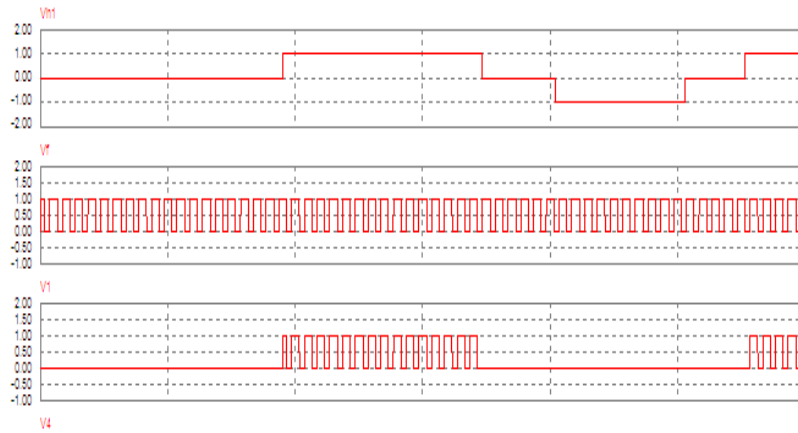


**Fig. 4.15 Deriving Gate pulses for switch1**

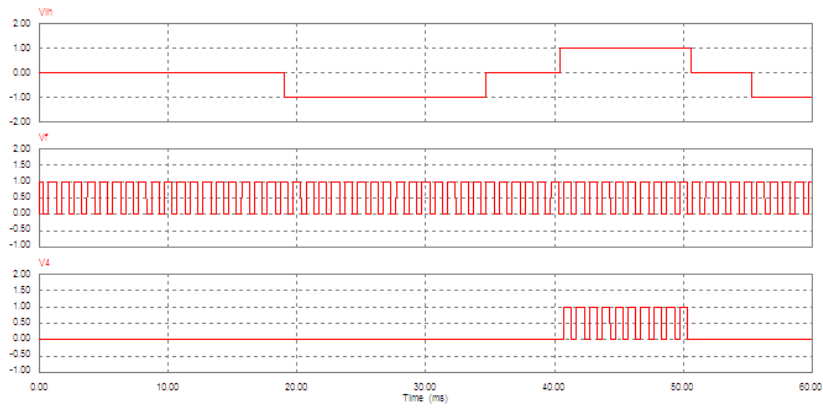


**Fig.4.16 Deriving Gate pulses for switch 4**

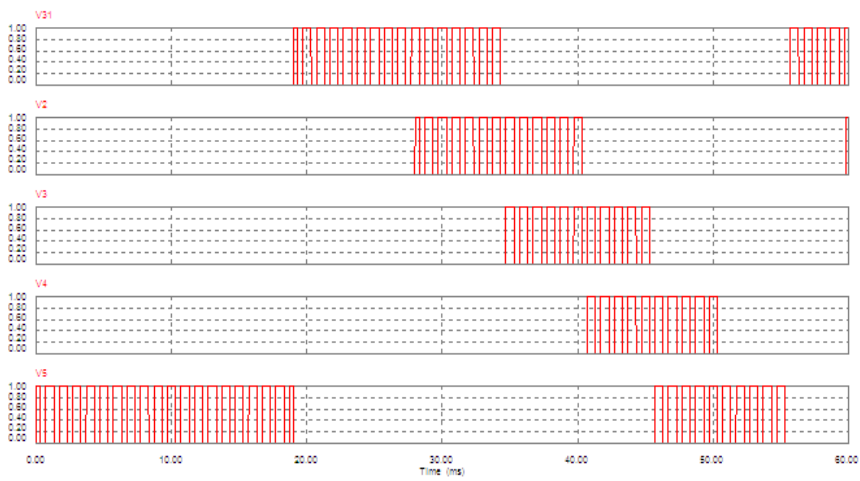


**Fig.4.17 Gate pulses for Inverter switches**

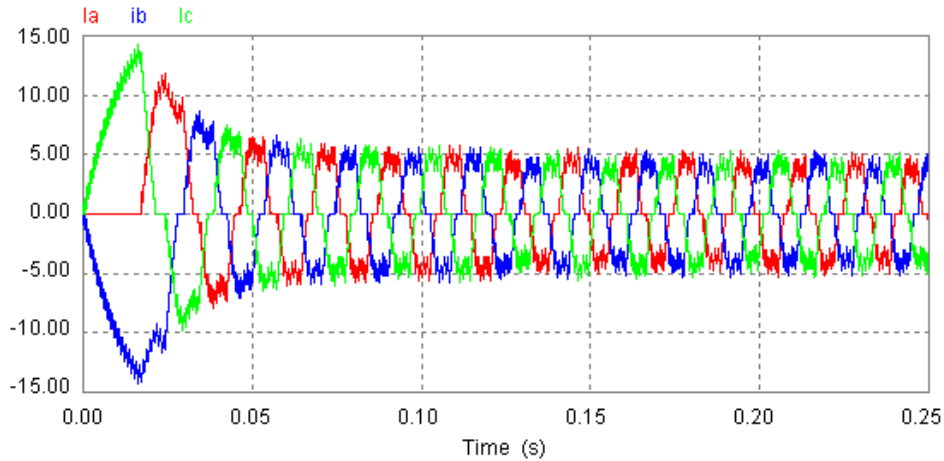


**Fig.4.18 Phase currents for PWM controlled PMBLDC Motor Drive**

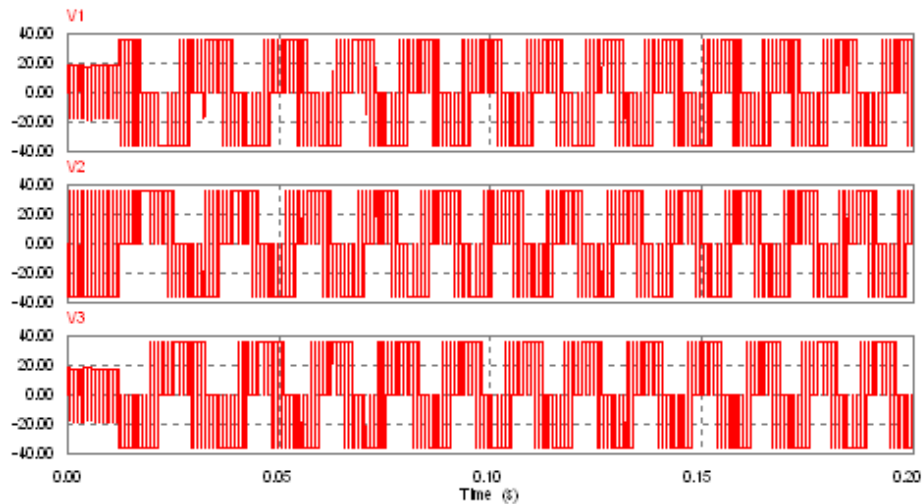


**Fig.4.19 Line voltages for PWM controlled PMBLDC Motor Drive**

The pulse width of the gate pulses is varied as the level (amplitude) of the accelerator signal varies. The variation in the pulse width is used to control the speed of the drive. As the accelerator signal is varied from 4.8V to 0 V, the speed of the motor reduces from a maximum of 190 *r.p.m.* to zero, for a load torque of 0.6 N-m. The stator current is also observed to reduce from its maximum value of 10 Amp, with the reduction in the pulse width. However the maximum value of the stator voltages remains the same. The speed (*r.p.m.*), current (amp) and torque (N-m) waveforms for two different accelerator positions are as shown in Fig. 4.20 and Fig.4.21.

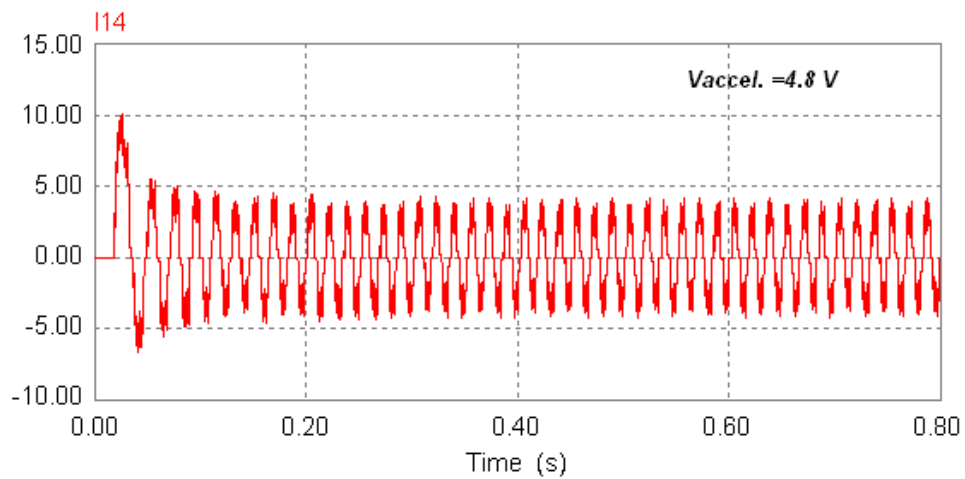
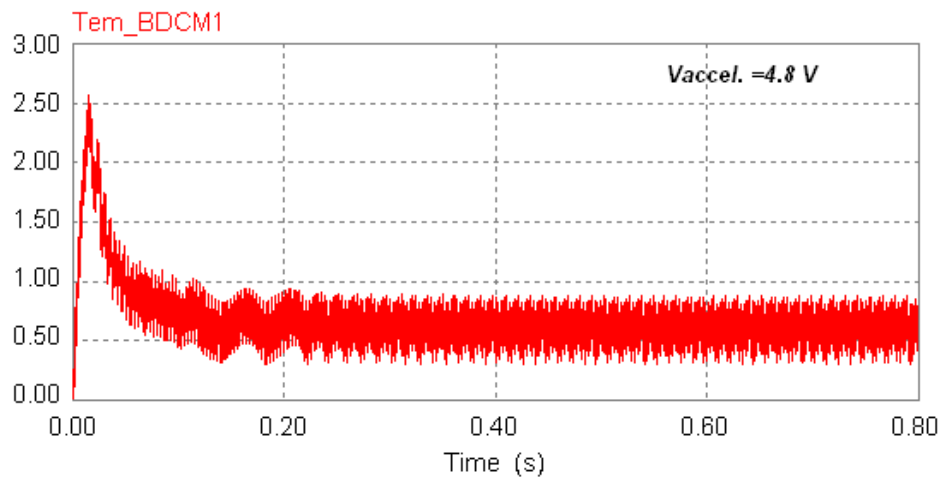
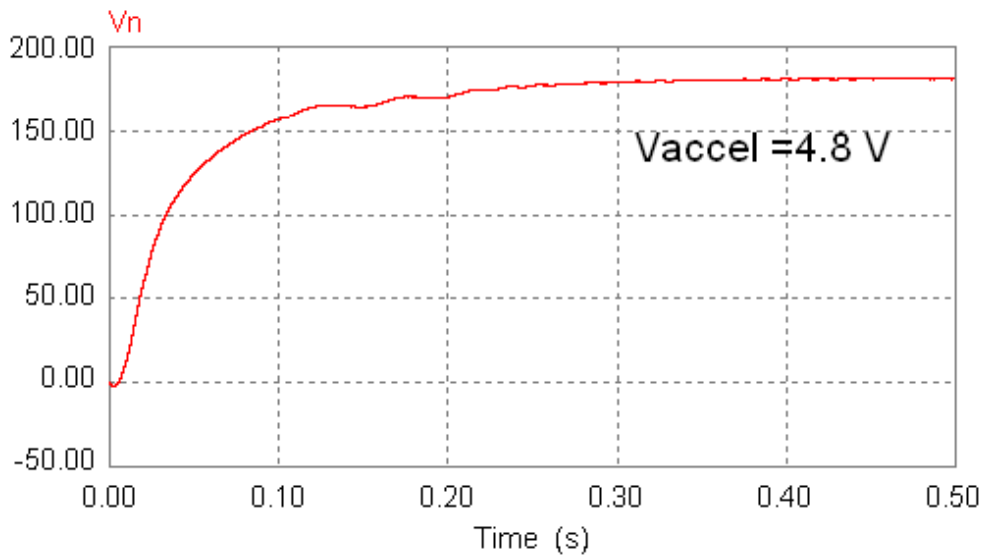


**Fig. 4.20 Speed, Torque and Phase current for PWM controlled PMBLDC Motor Drive (Vaccelerator =4.8V)**

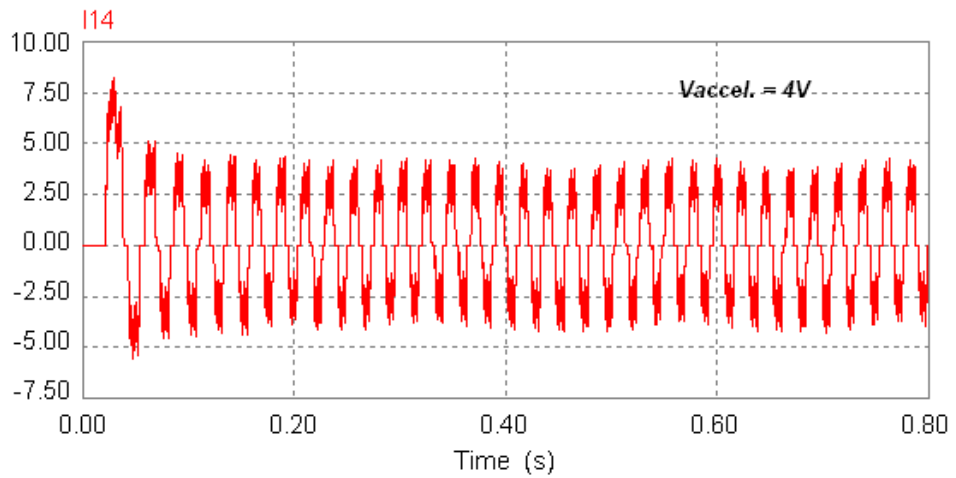
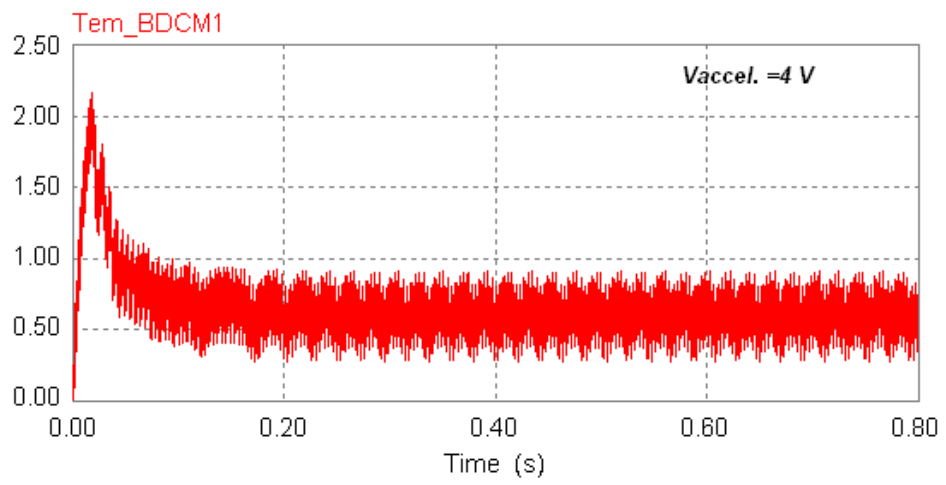
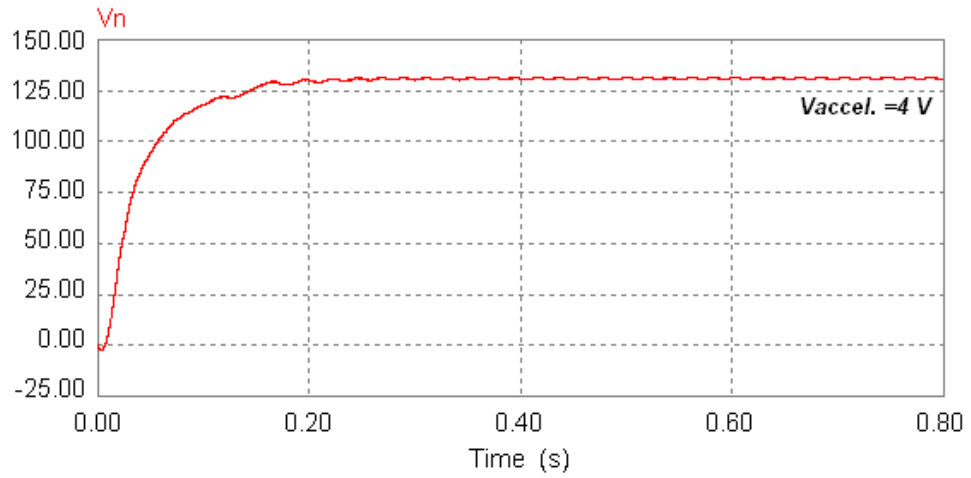


**Fig.4.21 Speed, Torque and Phase current for PWM controlled PMBLDC Motor Drive (Vaccelerator= 4V)**

## 4.6 Conclusions

It has been observed from the simulation results that as the accelerator signal is varied the pulse width and hence the speed of the motor varies. Hence the proposed control algorithm has been verified. Other important conclusions drawn from the Mathematical Modeling and simulation have been summarized are follows:

1. *abc* phase variable approach has been used for the mathematical model of BLDC Motor.
2. The trapezoidal back *e.m.f.* has been represented by Fourier series.
3. The open loop response of the BLDC indicates that it is an inherently stable system.
- 4 The motor speed and the phase currents have been found to vary with the variation in the amplitude of the accelerator signal.
5. The control logic has been validated by the simulation results.

## CHAPTER 5

# HARDWARE DEVELOPMENT FOR PWM CONTROLLED PMBLDC MOTOR DRIVE

### 5.1 General

The control logic has been implemented using discrete components. The control logic was first verified with a 3-phase resistive load (star connected 10 ohm, 500W). After the successful implementation, the load was replaced with the PMBLDC Motor and the control signals were derived from the Hall sensor output.

For resistive load the control signals for the MOSFET were derived using the PWM technique. The 3-phase sinusoidal currents (50Hz) were first converted to square waveforms, which mimic the Hall sensor output. The PWM signal was derived by comparing a 5V d.c. Signal with a triangle (1 kHz) obtained from an operational amplifier. The schematic of the control logic is shown in Fig.5.1

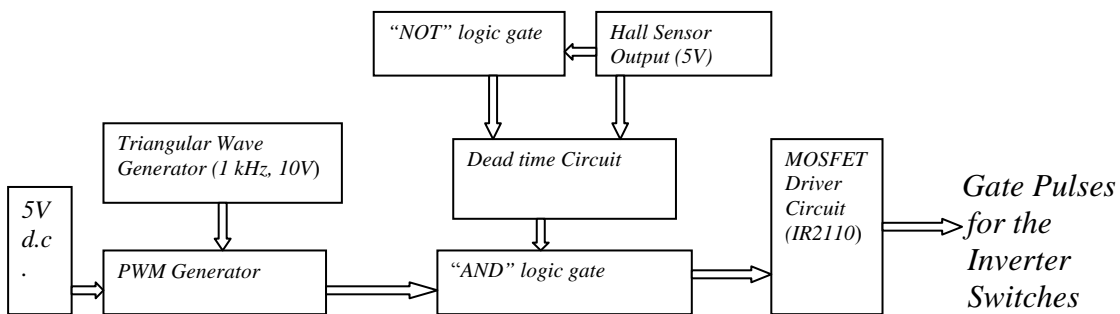


*Fig.5.1 Schematic of the control circuit*

### Development of Triangular wave generator.

The triangular signal has been used as a carrier signal to derive the PWM signal and has been generated by using the operational amplifier. To lower the switching losses of the inverter switches, the switching frequency has been taken to be 1 kHz. Since the magnitude of the accelerator signal varies from 4.3V to 0.8V, the carrier triangle signal has been designed for  $V_{sat} = \pm 5V$ . Hence the design parameters are

Frequency = 1 kHz, amplitude (p-p) = 10 V. with  $V_{sat} = \pm 5V$

Selecting  $C=0.05\mu F$ , and using the relations  $f = 1/2RC$  and  $R_c = 1.16R_2$  we get

$R_2 = 10k\Omega$ ,  $R_c = 11.6 k\Omega$  (using 20 k $\Omega$ ) pot

The generation of PWM signal is as shown in Fig.5.2

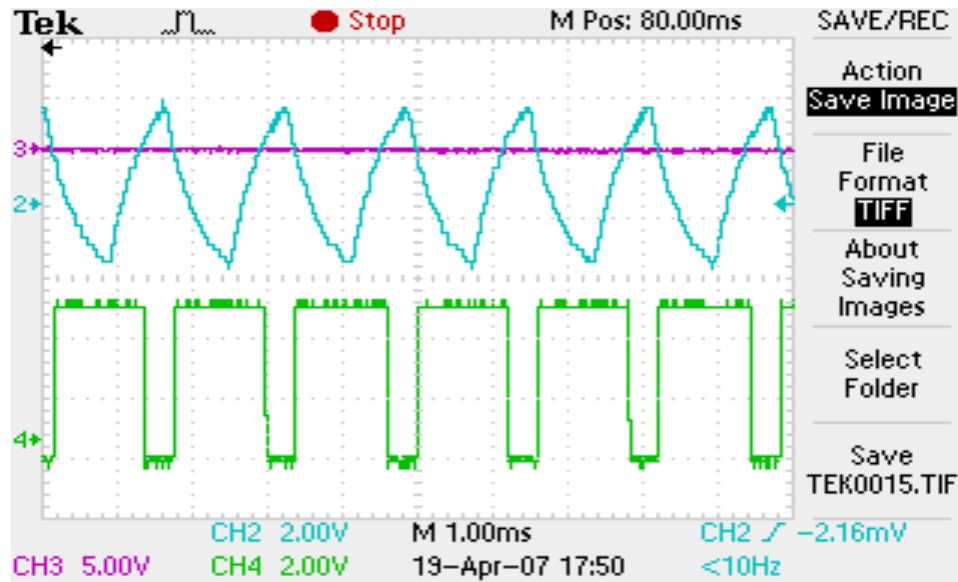


Fig. 5.1 Deriving the PWM signal-implementation

### 5.3 Selection of Switching Device

The speed control of the motor requires the voltage applied to the stator windings be varied. This can be obtained by any of the modulation techniques. Hence turning the power switching element “ON” and “OFF”, the voltage applied to the motor can be varied to control



the speed of the motor. The selection of power devices for EV propulsion is generally based on the requirements of voltage rating, current rating and the switching frequency. The two main choices for power-switching elements for motor drives are MOSFET and IGBT [17]. Both MOSFET and IGBT are voltage-controlled devices. So, the switching can be controlled by supplying a voltage to the gate of the device, instead of the current. It is very important to select an appropriate device for the drive; which requires a detailed comparison of the most recent devices available. A comparison between MOSFET and IGBT [17, 18] is shown in table 5

**Table- 5 Comparison between MOSFET and IGBT**

	<i>MOSFET</i>	<i>IGBT</i>
$P_{loss}$	$I_{rms} R_{ds-on}$	$I_{ave} V_{ce-sat}$
<b>Power Dissipation</b>	High	Low
<b>Switching Loss</b>	Low	High
<b>Preferred for</b>	V < 250 V	V > 1000V
<b>Cost</b>	Less	More

Since the battery voltage is 36V and the selected switching frequency is 1 kHz, MOSFET has been selected as the switching device.

IRFP240 that is characterized by the following parameters is the device of choice for the present work,

$$V_{dss} = 200V, R_{ds} = 0.18\Omega, I_d = 20Amp$$

#### **5.4 Development of Gate Driver for MOSFET.**

The devices from the transistor family differ from the devices of the thyristor family with respect to their input or device characteristics. In case of a thyristor, once it is triggered it continues to remain in the conduction state unless a current passing through it reduces to zero. However in case of transistors to keep them in conduction state a continuous base or

gate signal is required. The two fundamental categories for gate drive are high-side and low-side, High-side means that the source of the MOSFET can float between ground and the high-voltage power rail. Low-side means the source is always connected to ground.

The features of the various MOSFET Drivers [19] available have been compared in table.6

*Table - 6 Comparison between the various choices for the driver is as follows*

Feature	IR 21844	IR2130	IR2110
<i>Phase</i>	Single	Three	Single
<i>Dead time</i>	Included, programmable	Included, fixed	Not included
<i>Input</i>	$H_{IN}, L_{IN}$	$H_{IN}, L_{IN}$	$H_{IN}, L_{IN}$
<i>Output</i>	$H_O, L_O$	$H_O, L_O$	$H_O, L_O$
<i>Cost,module (INR)</i>	-	550	90
<i>Availability (in India)</i>	Not available	Rare	Easily available

Although IR 21844 is the first choice, but IR 2110 has been selected, considering the availability and the cost. The detailed Pin Diagram of the same is shown in Fig.5.3.

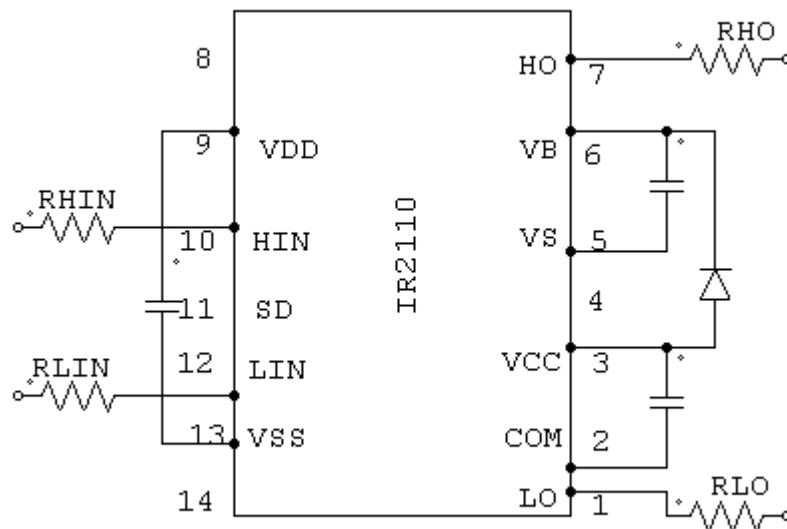


**Fig.5.3 Pin diagram of IR2110**

, $R_{Lin}= 2.7K \text{ Ohm}, R_{Hi}=10K \text{ Ohm}, R_{HO}=R_{LO}= 22 \text{ ohm}$

where  $R_{HIN}$  and  $R_{LIN}$  is the resistance at the input pins,  $R_{HO}$  and  $R_{LO}$  is the resistance at the output pins for the high side and the low side switch respectively.

### 5.5 Operation of Bootstrap Circuit

One significant feature of the MOS –gated transistors is their capacitive input characteristics. They are turned on by supplying a charge to the gate rather than a continuous current. Hence the isolated supply for the high side switch can be replaced by a capacitor. [14] The bootstrap supply is formed by a diode and capacitor. When  $V_s$  is pulled down to ground the bootstrap capacitor charges through the bootstrap diode from the 15V supply as shown in Fig.5.3.

### 5.6 Selection of Bootstrap Components

The bootstrap diode must be able to block the full voltage across the power rail. The current rating of the diode is the product of gate charge and the switching frequency. In order to reduce the charge feedback from the bootstrap capacitor into the supply, the fast recovery Diode is essential.

The voltage seen by the bootstrap capacitor is the  $V_{cc}$  supply only. Its capacitance is determined [20] by the equation;

$$Q_{bs} = 2Q_g + \frac{I_{qbs}}{f} + Q_{ls} + \frac{I_{cbs}}{f}$$

Where

$Q_g$ =Gate charge of high side MOSFET

$I_{cbs}$ =Bootstrap capacitor leakage current

$Q_{ls}$ = level shift charge required per cycle

The bootstrap capacitor must be able to supply this charge and retain its full voltage. Therefore the charge in the  $C_{bs}$  capacitor must be a minimum of twice the above value. The minimum capacitor value is calculated from the following equation;

$$C \geq \frac{2 \left[ 2Q_g + \frac{I_{qbs}}{f} + Q_{ls} + \frac{I_{cbs}}{f} \right]}{V_{cc} - V_f - V_{ls} - V_{min}}$$

Where:

$V_f$ = Forward voltage drop across the bootstrap diode

$V_{ts}$ =voltage drop across the low side MOSFET

$V_{min}$ =Minimum voltage between  $V_b$  and  $V_s$

As a rule of thumb the value obtained from the above equation should be multiplied by a factor of 15. Substituting the values of the parameters from the datasheets of the MOSFET and the gate driver IC.

The value of the bootstrap capacitor for IRFP240, at a switching frequency of 1 kHz comes out to be 100uF.

### 5.7 Dead Time Logic

The Hall Sensor output signal has been observed to have a conduction period of 180°. Therefore a dead time of 50µsec. has been between the complimentary switches of the same phase to avoid simultaneous switching of the devices. The dead time logic implemented is shown in Fig.5.4.

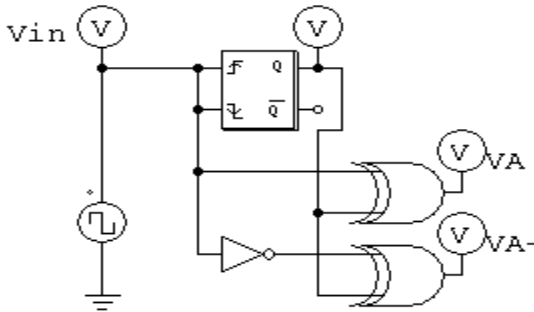
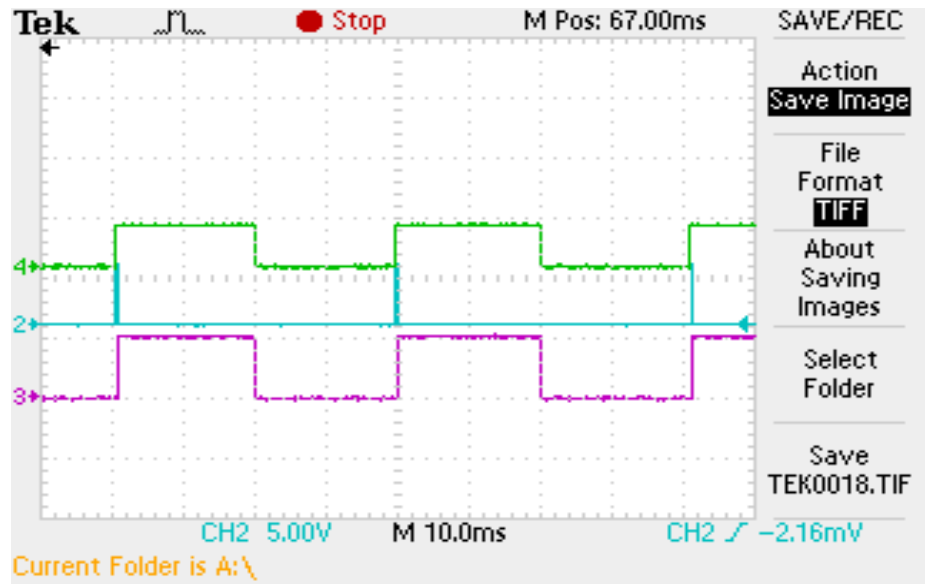


Fig. 5.4 Schematic of Dead Time logic

The waveforms obtained from the implementation are shown in Fig.5.5



*Fig.5.5 Dead Time between the complimentary switches-implementation*

### 5.8 Determination of the phase displacement of Hall sensors

The phase displacement and the phase sequence of the Hall sensors have been determined by manually rotating the motor and observing the Hall output on the oscilloscope. The displacement between the Hall sensors is found to be  $120^\circ$  as shown in Fig.5.6

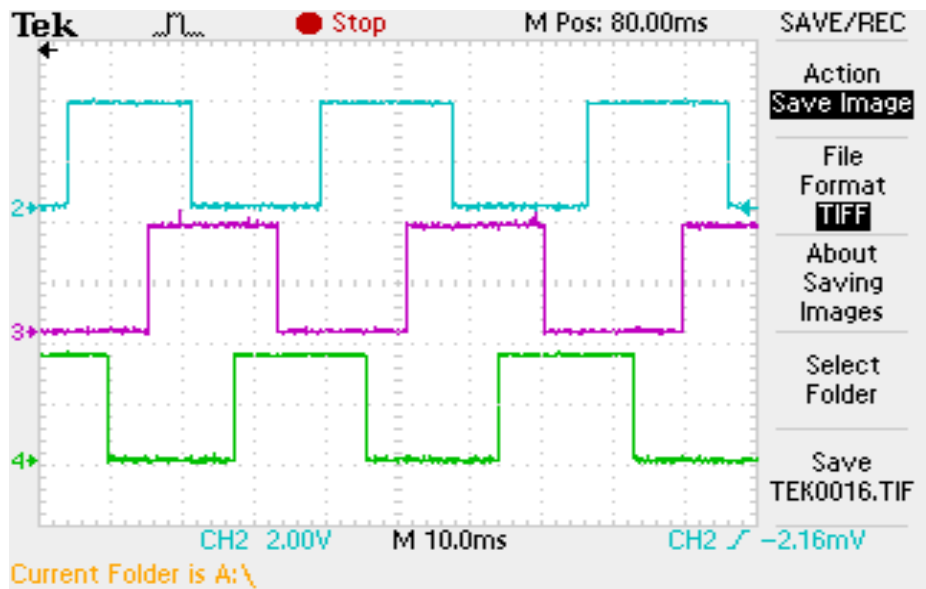


*Fig.5.6 Hall position sensor output of the PMBLDC Motor*

## **5.9 Conclusions**

The major observations made during the hardware development have been summarized as:

1. Since the switching losses and the cost of MOSFET is less as compared to the IGBT, MOSFET IRFP240 has been used as the switching device.
2. IR2110 has been used as the driver for high side and low side switches of the inverter.
3. Bootstrap capacitor of 100uF has been used to provide charge to the high side switch.
4. A dead band of 50μsec. has been provided between the two complimentary switches of the same leg.
5. The phase displacement between the Hall position sensors of the PMBLDC Motor is found to be 120°.

## CHAPTER 6

---

### PERFORMANCE OF PWM CONTROLLED PMBLDC MOTOR DRIVE

#### 6.1 General

The control circuit and the power module have been developed. The waveforms and the observed results for the inverter with resistive load and with PMBLDC Motor are discussed.

#### 6.2 Execution and Development of the Control Circuit

The control circuit and the wave forms observed during the execution are shown as follows:

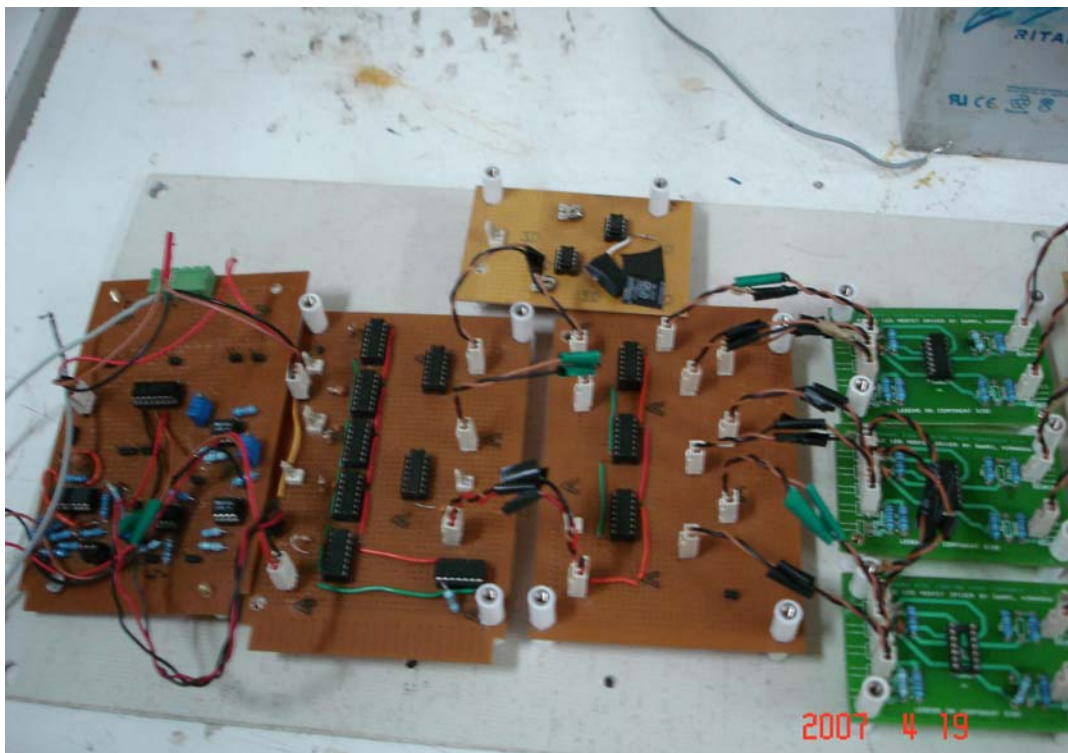


*Fig.6.1 The developed Control circuit for PWM controlled PMBLDC Motor*

The PWM signal derived and the Hall sensor output signal have been shown in Fig.5.2 and Fig.5.6 respectively.

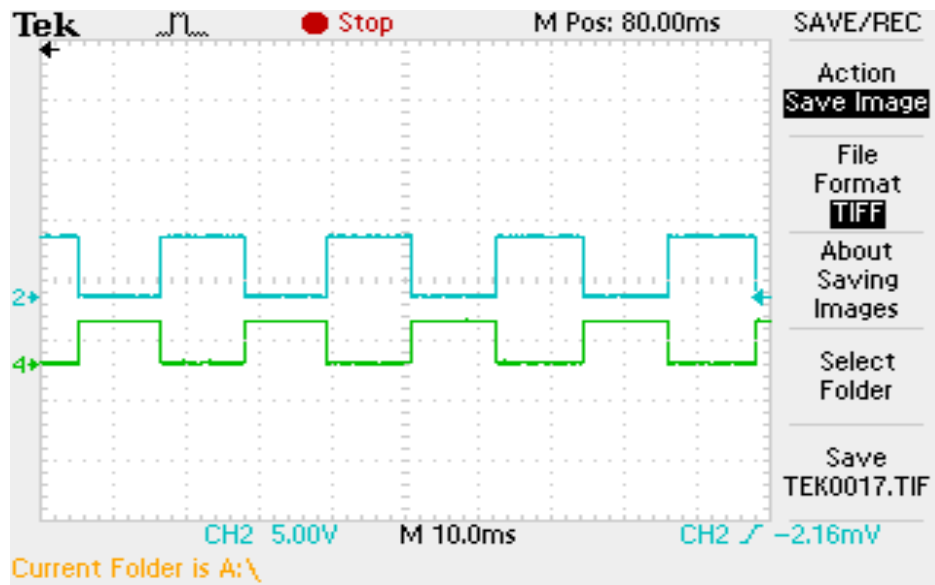


*Fig.6.2 Hall sensor output and the inverted signal for PMLDC Motor*

The dead time logic employed has been shown in Fig.5.5 and Fig.5.6. The pulse obtained at the output of the dead time circuit is shown in Fig. 6.3 and Fig.6.4

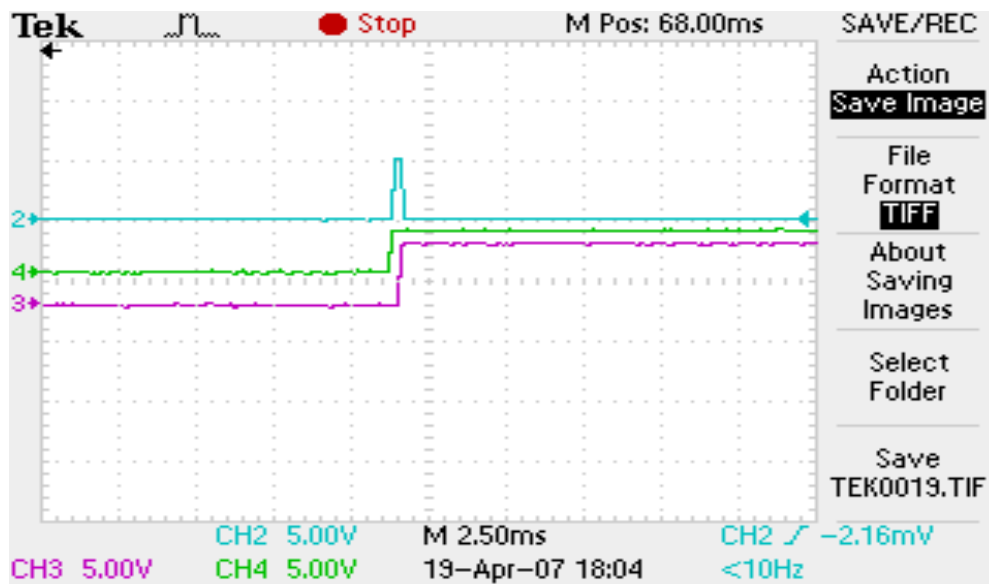


*Fig. 6.3 Generating dead time between complimentary Switches of the same leg*



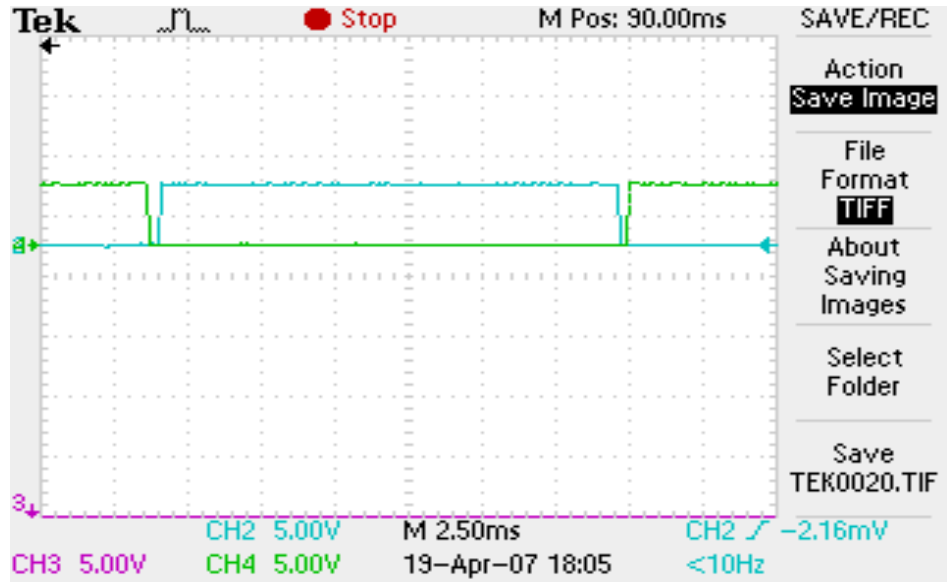


*Fig.6.4 Dead band between switches*

The gate pulses for the inverter switches have been derived by ANDing the PWM signal with the Hall sensor output signal; as shown in Fig.6.5

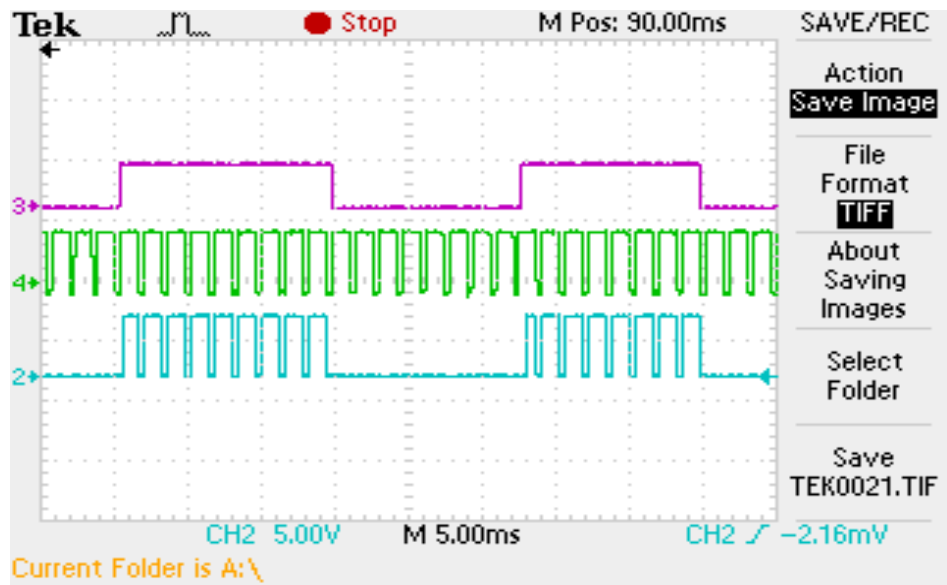


*Fig.6.5 Generating the gate pulse for inverter switches*

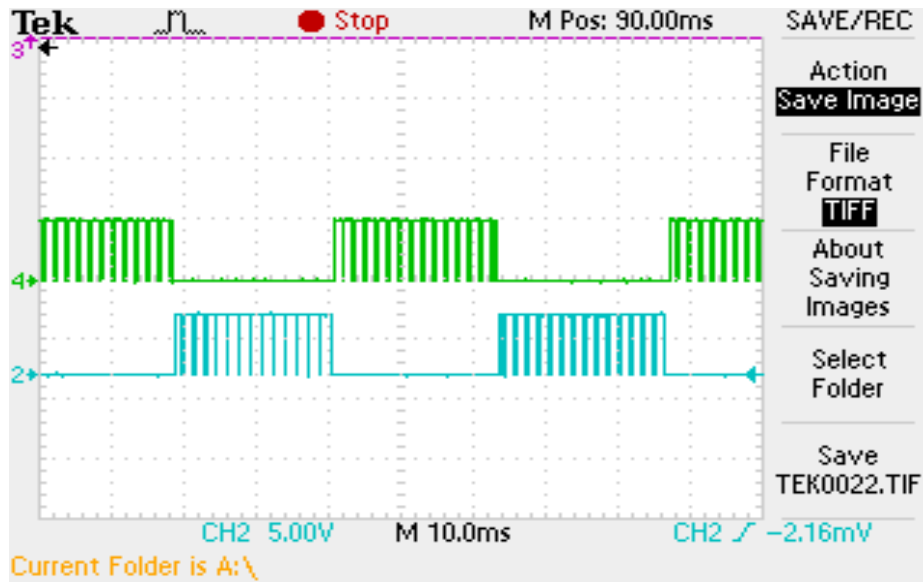


*Fig.6.6 Gate pulses for the complimentary switches at the MOSFET driver I/P (amplitude=5V)*

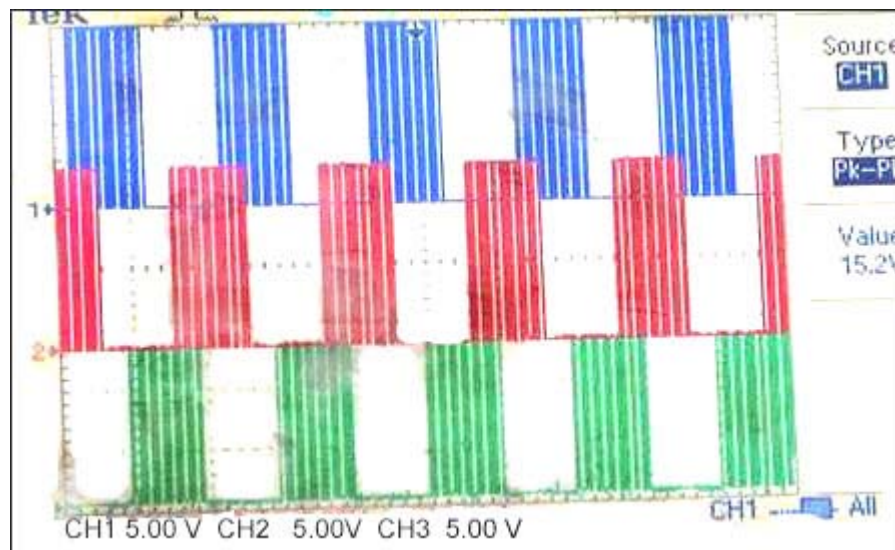


*Fig.6.7 Gate pulses for high side switches at the MOSFET driver O/P(amplitude=15V)*

### 6.3 Performance of the Inverter with Resistive Load

The power module has been fabricated by mounting six MOSFETs on the PCB, along with the heat sinks. Two 1000 $\mu$ F, 100V capacitors have been connected in parallel across the battery terminals to filter out the ripples in the input. The control signals for resistive load have been derived from a three phase transformer using a zero crossing detector circuit. A 5V dc supply has been used to derive the PWM signal.



*Fig.6.8 Control circuit and the power module for PWM controlled PMBLDC Motor*

The output of the inverter is found to vary with the variation in the modulation index, for modulation index of one the output waveform has been observed to be the conventional six step. The output voltage waveforms for a 3-phase resistive load is shown in Fig. 6.9 and Fig.6.10. The amplitude of the output voltage obtained for different values of battery voltage is given in table 7.

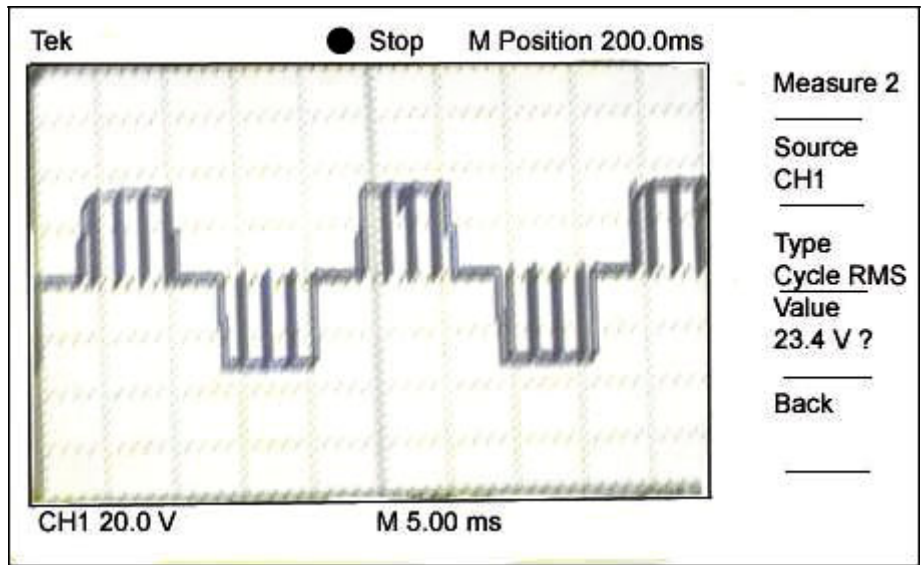


Fig.6.9 Line voltages for resistive load at battery voltage of 36V

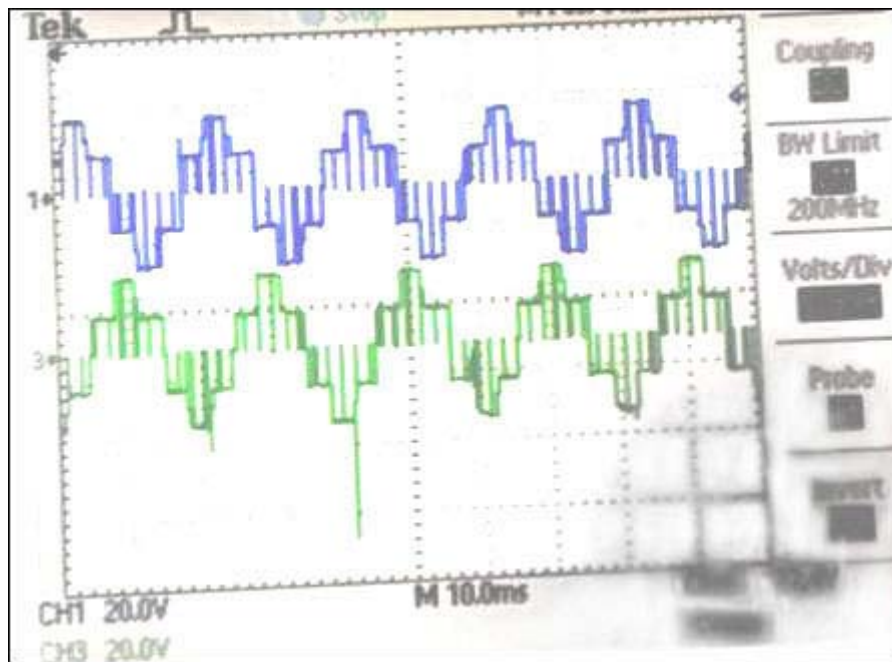
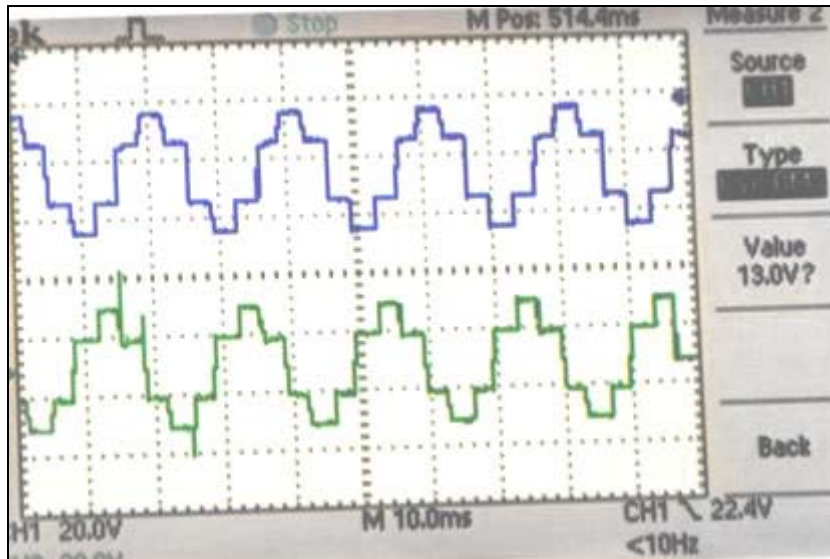


Fig.6.10 Phase voltages for resistive load at battery voltage of 36V

The *r.m.s.* value of the output voltage is varied with the change in the modulation index. The waveshape for a modulation index of one is shown in Fig.6.11



*Fig.6.11 Phase voltages for resistive load, at 36 V and modulation index=1*

*Table-7 Observed Inverter output at different battery voltages*

<i>Battery Voltage (V)</i>	<i>Line Voltage (V)</i>	<i>Phase Voltage (V)</i>
12	V <sub>p-p</sub> =24	V <sub>p-p</sub> =18
	V <sub>r.ms(max)</sub> .=9.31	V <sub>r.ms(max)</sub> .=5.32
24	V <sub>p-p</sub> = 48	V <sub>p-p</sub> = 25
	V <sub>r.ms(max)</sub> .=14.6	V <sub>r.ms(max)</sub> .=10.6
36	V <sub>p-p</sub> = 71	V <sub>p-p</sub> =46
	V <sub>r.ms(max)</sub> .=23.5	V <sub>r.ms(max)</sub> .=13.4

#### **6.4 Performance of the Inverter with the PMBLDC Motor used for Electric Vehicle**

The speed of the motor has been found to vary with the change in the accelerator position. The maximum speed observed at no load is 387 *r.p.m*, which can be reduced to zero by varying the accelerator position. The observed output voltage waveform is distorted; also the motor operation is mitigated by high acoustic noise, which is result of the switching

strategy employed. The motor speed obtained and the experimental set up is shown in table 8 and Fig.6.12 respectively.

*Table -8 Motor speeds at different values of stator voltage.*

<i>S.NO</i>	<i>Stator Voltage(V)</i>	<i>Rotor Speed(r.p.m.)</i>
1.	55.4	350
2.	59	366
3.	61.6	387



*Fig 6.12 Complete experimental set-up of PWM controlled PMSLDC Motor Drive for Electric Vehicle*

## **6.4 Conclusions**

The control algorithm proposed has been verified with the PMBLDC motor at no load, other important conclusions drawn from the observed waveforms and results have been briefly summarized as:

1. The inverter output is satisfactory for resistive load.
2. The speed of the motor varies as the pulse width is varied.
3. The voltage waveform for PMBLDC is distorted.
4. High acoustic noise is observed during the operation of the motor.

## CHAPTER 7

---

### MAJOR CONCLUSIONS AND SCOPE FOR FUTURE WORK

#### 7.1 General

The proposed control algorithm has been simulated, developed and validated by the experimental results. The maximum speed of the motor is observed to be 387 *r.p.m.*, at no load. Major conclusions drawn from the present work are discussed.

#### 7.2 Major Conclusions

The major conclusions drawn during the literature survey and the execution of the entire project have been summarized as:

- PMBLDC Motor is being by most of the popular brands of Electric Vehicles.
- PMBLDC Motor is characterized by trapezoidal back *e.m.f.* and requires rectangular currents to produce positive torque.
- The required current profile can be achieved by using either a voltage source inverter or a current source inverter as a power converter for the drive.
- Rotor position feedback is essentially required to synchronize the phase currents and the back *e.m.f.*
- It is observed from the open loop response that BLDC Motor is an inherently stable system.
- The proposed control algorithm has been supported by simulation results which indicate that as the accelerator position is varied the speed as well as the stator phase current changes.
- Bootstrap principle reduces the need for a separate supply for the high side switch.
- The performance of the inverter is validated using the resistive load.
- The inverter output possess voltage spikes which are present due to;
  - The wiring inductances
  - The circuit layout



- High acoustic noise has been observed in the motor output, which is the result of the switching strategy used, as only one switch per phase is being modulated in a cycle.

## **7.2 SCOPE FOR FUTURE WORK**

- Incorporating thermal and under voltage protection features for the developed controller.
- Adding current limiting feature to the control strategy.
- Increasing the switching frequency and analyzing the results.

## REFERENCES

- [1]. C.C.Chan “The State of the art of Electric and Hybrid Vehicles” proceedings of the IEEE Vol: 90, No.2, February 2002
- [2]. C.C.Chan “The State of the ART of Electric and Hybrid Vehicles” proceedings of the IEEE Vol: 90, No.2, February 2002
- [3]. C.C.Chan “An overview of power electronics in Electric Vehicles” IEEE transactions on Industrial Electronics Vol: 44, No1, February 1997.
- [4]. “DC-DC Converter Current Source fed Naturally Commutated Brushless DC Motor Drive” M.Tech thesis by Rahul Kumar Khopker. Texas & AM University.
- [5]. “Battery Assisted Bicycle” Ravinder Naik, M.Tech thesis, IISC, Bangalore
- [6]. H.Tan, S.L.Ho, “A Novel Single Sensor Technique Suitable for BLDCM Drive.” IEEE 1999 International Conference on Power Electronics and Drive system, PEDS, July 1999, Hong-Kong.
- [7]. G.H.Kim, J. Kang, J.S.Won “Analysis of the Commutation Torque Ripple Effect for BLDCM fed by HCRPWM –VSI.” IEEE Transactions on Power Electronics, 1992 pp.277-284
- [8]. T. Gopalarathnam, “New solutions for improved unipolar-excited brushless motor drives”, Ph.D. dissertation, Texas A&M University, College Station, TX, May 2002
- [9]. Bhim Singh, B.P. Singh M Kumar “PFC Converter fed PMBLDC Motor Drives for Air Conditioning” IE(I) Journal-EL, May 2001
- [10]. C.C Chan, J.Z. Jiang, X.Y. WANG, and K.T Chau, “Novel Polyphase Multipole Square-wave Permanent Magnet Motors Drive for Electric Vehicle.” IEEE transaction on Industry Applications, vol: 30, 1994, pp.1258-1266.
- [11]. Z.Q. Zhu, Y.Liu, D.Howe “Comparison of Performance of Brushless DC Drives Under Direct Torque Control and PWM Current Control”
- [12] “Power Loss Estimation in BLDC Motor Drives Using iCalc” Application Note AN-1048, International Rectifier

- [13]. "Control Tutorials for MATLAB and Simulink", from mathcentral.com
- [14]. P.Pillay and R.Krishnan,"Modeling of Permanent Magnet Motor drives."IEEE Transaction on Industrial electronics. Vol: 35, No.4, November, 1988.
- [15]. R. Somanatham, P.V.N. Prasad, A.D. Rajkumar "Modeling and Simulation of sensorless Control of PMSBLDC Motor Using Zero –Crossing Back E.M.F Detection."SPEEDAM 2006
- [16]. P.Pillay and R.Krishnan "Modeling,Simulation,and Analysis of Permanent –Magnet Drives, PartII:Thee Brushless DC Motor Drive"IEEE Transactions on Industry Applications,Vol:25, No.2,March/April 1989
- [17]. "Determining MOSFET Driver Needs for Motor Drive Applications"AN-898, Application Note, Microchip Technology Inc
- [18]. "IGBT or MOSFET: Choose Wisely" by Carl Blake and Chris Bull, International Rectifier
- [19]. "MOSFET/IGBT Drivers" International Rectifier
- [20]. "HV Floating MOS-Gate Driver ICs" Application NoteAN-978, International Rectifier
- [21]. "Bootstrap Component Selection for Control IC's", DT98, Design Tip, International Rectifier.
- [22]. S.K. Safi, P.P.Acarney , A.G. Jack "Analysis and Simulation of the high –speed torque performance of brushless DC motor drives"IEE Proceedings on Power Applications, Vol: 142,No.3, May 1995..
- [23]. S.D.Sudoff, P.C.Krause "Operating Modes of the Brushless dc Motor with a 120 inverter"IEEE transaction on energy conversion,Vol: 5 ,No.3 September 1990.
- [24]. T. Gopalarathnam, "New Solutions for Improved Unipolar-excited Brushless Motordrives", Ph.D. dissertation, Texas A&M University, College Station, TX, May2002.
- [25]. H.A. Toliyat, N. Sultana, D.S. Shet, and J.C. Moreira, "Brushless permanent Magnet (BPM) motor drive system using load-commutated inverter", IEEE Trans. On Power Electronics, Vol: 14, No. 5, September. 1999, pp. 831-837.

- [26]. R.Krishnan “A Novel Single –Switch –Per-Phase Converter Topology for Four – quadrant PM Brushless DC Motor Drive”.
- [27]. Chan CC, Xia W, Jiang JZ, Zhu ML. “Permanent magnet Brushless Drives”. IEEE Industry application magazine. Nov/Dec 1998.
- [28]. Humid A. Toliyat, Tilak Gppalarathnam. “A.C.Machines Controlled as D.C Machines.”
- [29]. Padmaraja Yedamale, “Brushless Motor Fundamentals”, Microchip technology Inc.
- [30]. Ramakant A. Gayakwad”Op-Amps and Linear Integrated Circuits”.
- [31]. all datasheets .com

## APPENDIX

### I. Specifications of the Motor under Study.

Speed: 195 *r.p.m.*

Voltage rating: 36V

Power rating: 250W

No. of poles: 40

No. of Phases: 3

Displacement of Hall elements: 120 °

### II. Fourier Series representation of the trapezoidal back *e.m.f*

The Fourier series for a function  $f(x)$  is given by:

$$F = a_0 + \sum_1^{\infty} [a_n \cos nx + b_n \sin nx]$$

$$\text{where } a_0 = \frac{1}{\pi} \int_0^{2\pi} f(x) dx ;$$

$$a_n = \frac{1}{\pi} \int_0^{2\pi} f(x) \cos nxdx ;$$

$$\text{and } b_n = \frac{1}{\pi} \int_0^{2\pi} f(x) \sin nxdx ;$$

For trapezoidal waveform, the above parameters can be calculated to get

$$a_0 = 0 ; \quad a_n = 0 ;$$

$$b_n = \frac{8}{\pi^2} \left[ \frac{\sin(n\pi/4) + \sin(3n\pi/4)}{n^2} \right] ;$$

Hence the trapezoidal back *e.m.f.* can be represented as:

$$E(\theta) = \sum_1^{\infty} \frac{8}{\pi^2} \left[ \frac{\sin(n\pi/4) + \sin(3n\pi/4)}{n^2} \right] \sin n\theta$$

where  $\theta$  varies from 0 to  $2\pi$